
A SEMI-SUPERVISED BAYESIAN MIXTURE MODELLING APPROACH FOR JOINT BATCH CORRECTION AND CLASSIFICATION

STEPHEN COLEMAN^{*,1}, KATH NICHOLLS^{1,2},

XAQUIN CASTRO DOPICO³, GUNILLA B. KARLSSON HEDESTAM³,

PAUL D.W. KIRK^{†,1,2,4}, CHRIS WALLACE^{†,1,2}

¹ MRC Biostatistics Unit, University of Cambridge, U.K.

² Cambridge Institute of Therapeutic Immunology & Infectious Disease, University of Cambridge, U.K.

³ Department of Microbiology, Tumor and Cell Biology, Karolinska Institutet, Sweden.

⁴ Cancer Research U.K. Cambridge Centre, Ovarian Cancer Programme, University of Cambridge, U.K.

1

ABSTRACT

2 Systematic differences between batches of samples present significant challenges when
3 analysing biological data. Such *batch effects* are well-studied and are liable to occur in
4 any setting where multiple batches are assayed. Many existing methods for accounting
5 for these have focused on high-dimensional data such as RNA-seq and have assumptions
6 that reflect this. Here we focus on batch-correction in low-dimensional classification prob-
7 lems. We propose a semi-supervised Bayesian generative classifier based on mixture mod-
8 els that jointly predicts class labels and models batch effects. Our model allows obser-
9 vations to be probabilistically assigned to classes in a way that incorporates uncertainty
10 arising from batch effects. By simultaneously inferring the classification and the batch-
11 correction our method is more robust to dependence between batch and class than pre-
12 processing steps such as ComBat. We explore two choices for the within-class densities:

* Corresponding author: stephen.coleman@mrc-bsu.cam.ac.uk

† These authors provided an equal contribution.

A semi-supervised Bayesian mixture modelling approach for joint batch correction and classification

the multivariate normal and the multivariate t . A simulation study demonstrates that our method performs well compared to popular off-the-shelf machine learning methods and is also quick; performing 15,000 iterations on a dataset of 750 samples with 2 measurements each in 11.7 seconds for the MVN mixture model and 14.7 seconds for the MVT mixture model. We further validate our model on gene expression data where cell type (class) is known and simulate batch effects. We apply our model to two datasets generated using the enzyme-linked immunosorbent assay (ELISA), a spectrophotometric assay often used to screen for antibodies. The examples we consider were collected in 2020 and measure seropositivity for SARS-CoV-2. We use our model to estimate seroprevalence in the populations studied. We implement the models in C++ using a Metropolis-within-Gibbs algorithm, available in the R package `batchmix`. Scripts to recreate our analysis are at <https://github.com/stcolema/BatchClassifierPaper>.

Keywords SARS-CoV-2 · ELISA · Mixture model · Batch correction · Bayes · Assay data · Classification.

1 Background

Many biological assays are performed across sets of samples or *batches*. When the number of samples exceeds the batch size, then it is common to notice *batch effects*, systematic differences between assay readouts from different batches which may affect both their mean and scale. This is a prevalent problem, that may be addressed in a variety of ways depending on the planned downstream analysis. In discussing available options for batch correction, we will use the term “batch effect” to mean differences between samples arising from between-batch technical factors in the experiment, and the term “class effect” to refer to biological differences arising due to samples coming from distinct biological classes. We consider settings in which the objective is to classify unlabelled samples into predefined classes.

To analyse class effects we should also account for the batch effects. One common approach is to first correct for batch effects as part of a pre-processing or data cleaning step (which might be as simple as zero-centring the data; i.e., transforming each batch to have a common mean), and then to apply standard classification models to the resulting “cleaned” data (e.g., 2, 27, 36). However, such two-step approaches have been found to increase false positive rates because they may induce correlation between the cleaned observations which is typically not accounted for in downstream analysis (25). Further, when batch is confounded with class effects (due to unbalanced representation of classes across batches) then naive adjustment which ignores known biological classes in the data can lead to incorrect conclusions (23), and methods for adjustment

A semi-supervised Bayesian mixture modelling approach for joint batch correction and classification

43 which preserve differences attributable to known classes can lead to false positive results (32). An alternative
44 approach is to incorporate batch information directly into downstream analyses, for example as a covariate in
45 regression-based approaches. It has been shown that mixed effects models which share information between
46 batches produce better calibrated quantitative data than independent analyses of each batch (39). However,
47 only a subset of analytical approaches have been adapted to accommodate batch effects (e.g., 31, 33, 22),
48 and there has been a strong focus on high-dimensional settings (e.g., 18, 6, 1). Thus a need exists for a wider
49 range of methods that can account for batch effects directly in low-dimensional data analysis.

50 Here we focus on the problem of assigning class labels using low-dimensional assay data generated across
51 several batches. This is a common design in many assays that measure a small number of specific biomark-
52 ers such as enzyme-linked immunosorbent assay (ELISA) and flow cytometry data. If there are known
53 classes in the population, then class-specific controls can be included in the assay, resulting in training ex-
54 amples for which the class labels are known. We are motivated in part by the specific problem of estimating
55 seroprevalence of SARS-CoV-2 by classifying individuals into seropositive and seronegative classes at dif-
56 ferent points in time during the pandemic. Since batches tend to comprise samples collected at the same
57 time point, and since seroprevalence is expected to vary through the course of the pandemic, we expect
58 class membership to be imbalanced across batches – motivating the development of a joint classification
59 and batch-correction model, rather than a 2-step approach. Insofar as we are aware, there is no appropriate
60 method for classification using data with all of these characteristics.

61 To address this, we propose a semi-supervised Bayesian mixture model that explicitly models batch param-
62 eters and predicts class membership. Our method is semi-supervised as our model parameters are inferred
63 using both the labelled and unlabelled data. In an iteration of our MCMC algorithm the unobserved class
64 labels are inferred, then a subset of the data, X_k , are associated with the k^{th} class, and X_k can be divided
65 into unlabelled (u) and labelled (l) data, e.g., $X_k = [X_{(l)k}, X_{(u)k}]$, where the labels of $X_{(l)k}$ are observed
66 and the labels of $X_{(u)k}$ are imputed. The class parameters are then inferred conditioning on the entirety of
67 X_k . This happens in each iteration of our sampler and the algorithm is run for at least as many iterations
68 as it takes to converge. Semi-supervised Bayesian mixture models have had some success in biomedical
69 applications, e.g. Crook et al. (10, 11). The Bayesian framework also allows our model to propagate the
70 uncertainty arising from the batch effects to the class allocation probabilities for each item in the dataset.
71 This provides a more complete quantification of the uncertainty in the final predictions, thereby enabling
72 more informed interpretation.

73 This manuscript is organised as follows: in section 2 we describe our model; in section 3 we evaluate our
74 model using simulated data, and compare to off-the-shelf machine learning methods; in section 4 we com-

A semi-supervised Bayesian mixture modelling approach for joint batch correction and classification

75 pare the same set of models on a gene expression dataset where the true class is known and we simulate
 76 batch-effects under two scenarios; and in section 5 we apply the proposed method to two ELISA studies of
 77 seroprevalence of SARS-CoV-2 in Stockholm (7) (section 5.1) and Seattle (12) (section 5.3). We then con-
 78 clude our manuscript in section 6 with a discussion of the contribution, limitations, and possible extensions
 79 to our model.

80 2 Model

81 2.1 Notation

82 We consider a study that collects P measurements for each of N individuals to form a dataset $X =$
 83 (X_1, \dots, X_N) , where $X_n = [X_{n,1}, \dots, X_{n,P}]^\top$ for all $n \in \{1, \dots, N\}$. We assume that each individ-
 84 ual has an associated observed batch label $b_n \in \{1, \dots, B\} \subset \mathbb{N}$, where B is the total number of batches,
 85 and we write $b = [b_1, \dots, b_N]^\top$ for the collection of all N batch labels. Note that as each individual belongs
 86 to a single batch, we assume that all P measurements for each individual are part of the same batch. We
 87 wish to predict class labels for each individual, and write $c = [c_1, \dots, c_N]^\top$ for the collection of all class
 88 labels. We assume that the number of classes, K , is known, so that each $c_n \in \{1, \dots, K\}$. We assume that
 89 a subset of labels are observed and each class is represented in this subset.

90 2.2 Model specification

We use a K -component mixture model to describe the data X . The mixture model can be be written

$$p(X_n) = \sum_{k=1}^K \pi_k f(X_n | \theta_k) \quad \text{independently for each } n = 1, \dots, N, \quad (1)$$

where $\pi = [\pi_1, \dots, \pi_K]^\top$ is the vector of component weights, $f(\cdot)$ is a parametric density function, and θ_k are the parameters of the k^{th} component. We assume each component describes a single and distinct class in the population and use the class labels to rewrite the model

$$p(X_n | c_n = k) = f(X_n | \theta_k). \quad (2)$$

We then introduce batch-specific parameters, $z = (z_1, \dots, z_B)$ and expand $f(\cdot)$ to accommodate these. Then conditioning on the observed batch label we have

$$p(X_n | c_n = k, b_n = b) = f(X_n | \theta_k, z_b). \quad (3)$$

A semi-supervised Bayesian mixture modelling approach for joint batch correction and classification

91 We focus on continuous data where each measurement has support across the entire real line. We consider
 92 the multivariate t density (**MVT**, density denoted $f_t(\cdot)$) and the multivariate normal (**MVN**, density denoted
 93 $f_N(\cdot)$) as choices for f , but depending on the situation other choices could be more relevant and our model
 94 is not inherently restricted to these. We use $z_b = (m_b, S_b)$, choosing m_b to be a P -vector representing the
 95 shift in location due to the batch effects and S_b to be a scaling matrix. We assume the observed location of
 96 X_n is composed of a class-specific effect, μ_k , and a batch-specific effect, m_b , so $(X_n | c_n = k, b_n = b) =$
 97 $\mu_k + m_b + \epsilon_n$. Similarly we assume that the random noise, ϵ_n , is subject to class and batch specific effects
 98 Σ_k and S_b respectively.

More specifically, if we use a mixture of MVN densities, then our class parameters are $\theta_k = (\mu_k, \Sigma_k)$, where μ_k is the P -dimensional mean vector and Σ_k is the $P \times P$ covariance matrix. We assume

$$(X_n | c_n = k, b_n = b) \sim \mathcal{N}(\mu_k + m_b, \Sigma_k \oplus S_b). \quad (4)$$

We define the operator \oplus for a $P \times P$ matrix, A , and a diagonal matrix B of equal dimension, as:

$$A \oplus B := \begin{pmatrix} a_{1,1}b_{1,1} & a_{1,2} & a_{1,3} & \cdots & a_{1,P} \\ a_{2,1} & a_{2,2}b_{2,2} & a_{2,3} & \cdots & a_{2,P} \\ a_{3,1} & a_{3,2} & a_{3,3}b_{3,3} & \cdots & a_{2,P} \\ \vdots & \vdots & \vdots & \ddots & \vdots \\ a_{P,1} & a_{P,2} & a_{P,3} & \cdots & a_{P,P}b_{P,P} \end{pmatrix}. \quad (5)$$

Similarly for a mixture of MVT densities, we assume

$$(X_n | c_n = k, b_n = b) \sim t_{\eta_k}(\mu_k + m_b, \Sigma_k \oplus S_b). \quad (6)$$

99 where η_k is the class-specific degrees of freedom.
 100 In the likelihood function, only the combinations of the class and batch parameters, $\mu_k + m_b$ and $\Sigma_k \oplus S_b$,
 101 are identifiable, and the values of the class and batch specific effects are not. However, we assume that we
 102 have some prior information about the relative orders of magnitude of the class and batch effects and encode
 103 this in an informative prior, reducing the problem of identifiability with this additional constraint. If the
 104 magnitude of the between-batch variability is similar to or greater than the true biological effect, then we
 105 suspect that any analysis of such a dataset is untenable, or at least that the data are not appropriate for our
 106 model.

A semi-supervised Bayesian mixture modelling approach for joint batch correction and classification

The full hierarchical model can be found in section 1 of the supplementary material. Here we include the choice of prior distributions for the class and batch effects:

$$\mu_k, \Sigma_k | \xi, \kappa, \nu, \Psi \sim \mathcal{N} \left(\mu_k | \xi, \frac{\Sigma_k}{\kappa} \right) \mathcal{IW} (\Sigma_k | \nu, \Psi), \quad (7)$$

$$m_{b,p} | \lambda, \delta^2 \sim \mathcal{N} (0, (\lambda \delta)^2), \quad (8)$$

$$(S_b)_{p,p} | \alpha, \beta, S_{loc} \sim \mathcal{IG} (\alpha, \beta, S_{loc}), \quad (9)$$

$$\eta_k | \epsilon, \zeta \sim \mathcal{G} (\epsilon, \zeta) \quad (\text{if the MVT density is being used}). \quad (10)$$

107 \mathcal{IW} denotes the inverse-Wishart distribution, \mathcal{IG} denotes the inverse-Gamma distribution with a shape
 108 α , rate β and location S_{loc} , \mathcal{N} signifies the Gaussian distribution parameterised by a mean vector and a
 109 covariance matrix and \mathcal{G} denotes the Gamma distribution parameterised by a shape and rate. An empirical
 110 Bayes approach is used to set the hyperparameters for the class mean and covariance (details are included in
 111 section 2 of the Supplementary material, these follow the suggestions of 14). The δ^2 hyperparameter is set
 112 to the mean of the diagonal entries of the observed covariance in the data. S_{loc} is set to 1.0 to ensure that the
 113 likelihood covariance matrix remains positive semi-definite. For the MVT mixture model, we choose the
 114 hyperparameters of the degrees of freedom to be $\epsilon = 20$ $\zeta = 0.1$ in line with suggestions from Juárez and
 115 Steel (20). This uninformative prior does not restrict η_k to small values, and enables the MVT mixture model
 116 to approximate the MVN model if the data are truly Gaussian. The remaining hyperparameters (λ, α and β)
 117 are user-specified, and we explore the impact of different choices on the final inference in sections 5.1 and
 118 5.3. We investigate the impact of 3 different values for each of these parameters, reflecting an informative
 119 or constrained prior, a flexible, uninformed prior, and a choice in the middle-ground.

Sampling the batch and class parameters allows us to derive a batch-corrected dataset, Y , in each iteration. We define the p^{th} measurement for the n^{th} sample in Y as

$$(Y_{n,p} | c_n = k, b_n = b, \dots) = \frac{X_{n,p} - m_{b,p} - \mu_{k,p}}{\sqrt{(S_b)_{p,p}}} + \mu_{k,p}, \quad (11)$$

120 for all $n = \{1, \dots, N\}, p = \{1, \dots, P\}$. Note that Y will incorporate the uncertainty about the batch
 121 and class parameters, and the classification. This transformation is similar to the empirical Bayes batch
 122 correction suggested by Johnson et al. (19); however their method is a pre-processing step that is applied to
 123 each measurement in turn, whereas our model is jointly inferring class and batch effects and may be applied
 124 to the full dataset.

125 We perform inference using a Metropolis-within-Gibbs sampler as described in section 3 of the supplemen-
 126 tary material.

A semi-supervised Bayesian mixture modelling approach for joint batch correction and classification

127 **3 Simulations**

128 **3.1 Simulation design**

129 We wish to evaluate the performance of the MVN and MVT implementations of our model and compare
130 these to the popular machine learning methods random forest (**RF**, 5), probabilistic support vector machine
131 (**SVM**, 4) and logistic regression (without batch-correction, **LR**). We also compare our method to ComBat
132 (19, 24), a popular pre-processing batch-correction method. We apply ComBat to our data and then model
133 the resulting dataset with the MVN and MVT mixture models and logistic regression. Finally, we consider
134 the semi-supervised Bayesian mixture model with no batch-correction.

135 To achieve this, we generate 100 datasets in each of 9 different scenarios. In six of these, the data are
136 generated from a mixture of MVN distributions and in one scenario the data is generated from a mixture of
137 MVT distributions. In two scenarios, data are sampled from a mixture of Poisson distributions. This count
138 data is log-transformed and then Gaussian noise is added to ensure our model is strongly misspecified in the
139 density choice. For each simulation we generate both a “batch-free” and an observed dataset. In seven of
140 the scenarios, the data contains $P = 2$ measurements for each of $N = 750$ samples; in two scenarios we
141 consider a higher feature space of $P = 15$. In all scenarios we consider $B = 5$ batches and $K = 2$ classes.
142 The classes are not evenly represented, in seven scenarios the first class expected to contribute 75% of the
143 samples with the remainder drawn from the second class, and class is independent of batch (and therefore
144 a pre-processing step is expected to match our model). In two scenarios the class labels and batch of origin
145 are dependent and pre-processing is expected to skew the inference. The batches are all expected to have
146 equal numbers of samples except in the Varying batch size scenario. We randomly select which class labels
147 are observed, sampling uniformly across the data indices, $\{1, \dots, N\}$. We expect one quarter of the labels
148 to be observed, i.e. $\mathbb{E} \left(\sum_{n=1}^N \phi_n \right) = 0.25N = 125$. These labelled observations constitute the training set
149 for the off-the-shelf methods.

150 More specifically, the nine simulation scenarios are:

- 151 • Base case: the generic, base scenario; all other scenarios are variations of this, using the same
152 choices for all bar a subset of parameters, with this subset varied to define the specific scenario.
- 153 • Batch-free: similar to the Base case but no batch effects are present (i.e., $m_b = \mathbf{0}_P$, $S_b = \mathbf{I}$).
- 154 • Varying batch effects: the Base case with more variance among the batch effects.
- 155 • Varying class representation: the classes are imbalanced across batches, i.e, the expected proportion
156 of each class varies across batches (note that this is a slightly different generating model, the class

A semi-supervised Bayesian mixture modelling approach for joint batch correction and classification

157 weights are batch specific). The first two batches contain a larger proportion of samples from class
158 1, the third batch is balanced and the final two batches have a greater proportion of samples from
159 class 2.

- 160 • Varying batch size: rather than equally sized batches, the batches have varying proportions of the
161 total sample. The expected proportions are $\frac{1}{2}, \frac{1}{4}, \frac{1}{8}, \frac{1}{16}, \frac{1}{16}$.
- 162 • Multivariate t generated: the data are generated from a MVT mixture model rather than a MVN
163 mixture model.
- 164 • Log-Poisson generated: the data are generated from a Poisson mixture model, log-transformed and
165 then Gaussian noise is added.
- 166 • High-dimensional: $P = 15$ features are generated.
- 167 • Hardest: this combines the data-generating mechanism of the Log-Poisson generated scenario, the
168 class and batch dependency of the varying class representation scenario and the dimensionality of
169 the high-dimensional scenario.

170 A more detailed description of the generating models, along with visualisations of an example dataset for
171 each scenario, are provided in section 4 of the supplementary material.

172 We use implementations of the machine learning methods available in R (34). For the RF this is the
173 `randomForest` package (26), for the SVM we use the `kernlab` package (21), and for LR we use the
174 base implementation of LR contained in the `glm` function. We use the default parameters in each method,
175 bar the SVM where we set `prob.model = TRUE` to build a model for calculating class probabilities. The
176 default for a classification SVM in this package uses a Gaussian Radial Basis kernel function.

177 We use the data with observed labels as the training set for each of these methods and those with unobserved
178 labels as a test set. We record the time taken to train the model and to predict the outcome for the test set.

179 3.2 Results

180 We assessed within-chain convergence by calculating the Geweke statistic (16), and removed chains which
181 failed the diagnostic test. We then selected chains with the highest median complete log-likelihood as repre-
182 sentative for the simulation. We compared the models using the Brier score between allocation probability
183 across classes and the true class (figure 1 A). We found that our mixture model performed better or at least as
184 well as the ML methods across all two dimensional scenarios. When the data were generated from Gaussian
185 distributions, the performance of the two versions of the mixture model performed very similarly. The MVT
186 mixture model learned a large degree of freedom for each component, indicating that this behaves as an

A semi-supervised Bayesian mixture modelling approach for joint batch correction and classification

187 approximation of the Gaussian mixture model when appropriate (figure 2). In contrast, in the Multivariate t
188 generated scenario, the performance of the MVN mixture model had greater variation in performance than in
189 any other scenario. Figure 2 also shows that parameter estimates were consistent across chains. When there
190 was no dependency between batch and class, the pre-processing batch-correction, ComBat, was as effective
191 as the combined model (batchmix). However, when this dependency is introduced ComBat is problematic
192 in keeping with results from Leek et al. (23), Li et al. (25), whereas batchmix is better protected from this
193 confounding. batchmix performed poorly in the high-dimensional scenarios, but this is potentially a prob-
194 lem with the sampler or the choice of priors as the model is no less well specified than in the Base case
195 scenario. However, this shows that batchmix should not be casually applied in high-dimensional data.

196 We also wanted a sense of how well our models would estimate the proportion of the classes in our simu-
197 lations as an analogue to seroprevalence in our motivating example. We recorded the predicted proportion
198 of the smaller class in the dataset, and compared the models' estimate to the truth (figure 1 B). We found
199 that the mixture models have a more narrow range in their estimates than the other models in the Base
200 case, No batch effects, Varying batch effects and Varying batch size scenarios, with a similar range for the
201 MVT mixture model in the other low-dimensaional scenarios indicating a more consistent behaviour than
202 the other methods. The MVN mixture model exhibited good behaviour, except when misspecified as in the
203 MVT generated data. We note that the mixture model's median performance is either an under-estimate of
204 the proportion of samples from the smaller class or to be centred on the true value. We also observed that
205 when the batch effects were more varied and greater in magnitude, the SVM and RF had very long tails in
206 their performance (Varying batch effects in figure 1 B).

207 The machine learning approaches and ComBat are all exceptionally fast, running in under a second. Running
208 the MCMC for batchmix to converge took longer but was still reasonable. In the Base case scenario, 25,000
209 iterations had a median runtime of 11.7s for the MVN model and 14.7s for the MVT model. Full time results
210 can be seen in figure 11 of the supplementary material.

211 4 Gene expression data

212 We consider a gene expression dataset for sorted peripheral blood cells (28) as an additional validation of
213 the model. The dataset contains 84 CD14 cells, 24 CD16, 17 CD19, 24 CD4, and 25 CD8 cells. There are
214 an additional unseparated 68 peripheral blood mononuclear cells (PBMC). We use the data as represented
215 in the first four principal components to reduce the dimensionality of the data. We then scale the features by
216 mean-centring them and transforming them to unit variance. We (artificially) introduce batch-effects under

A semi-supervised Bayesian mixture modelling approach for joint batch correction and classification

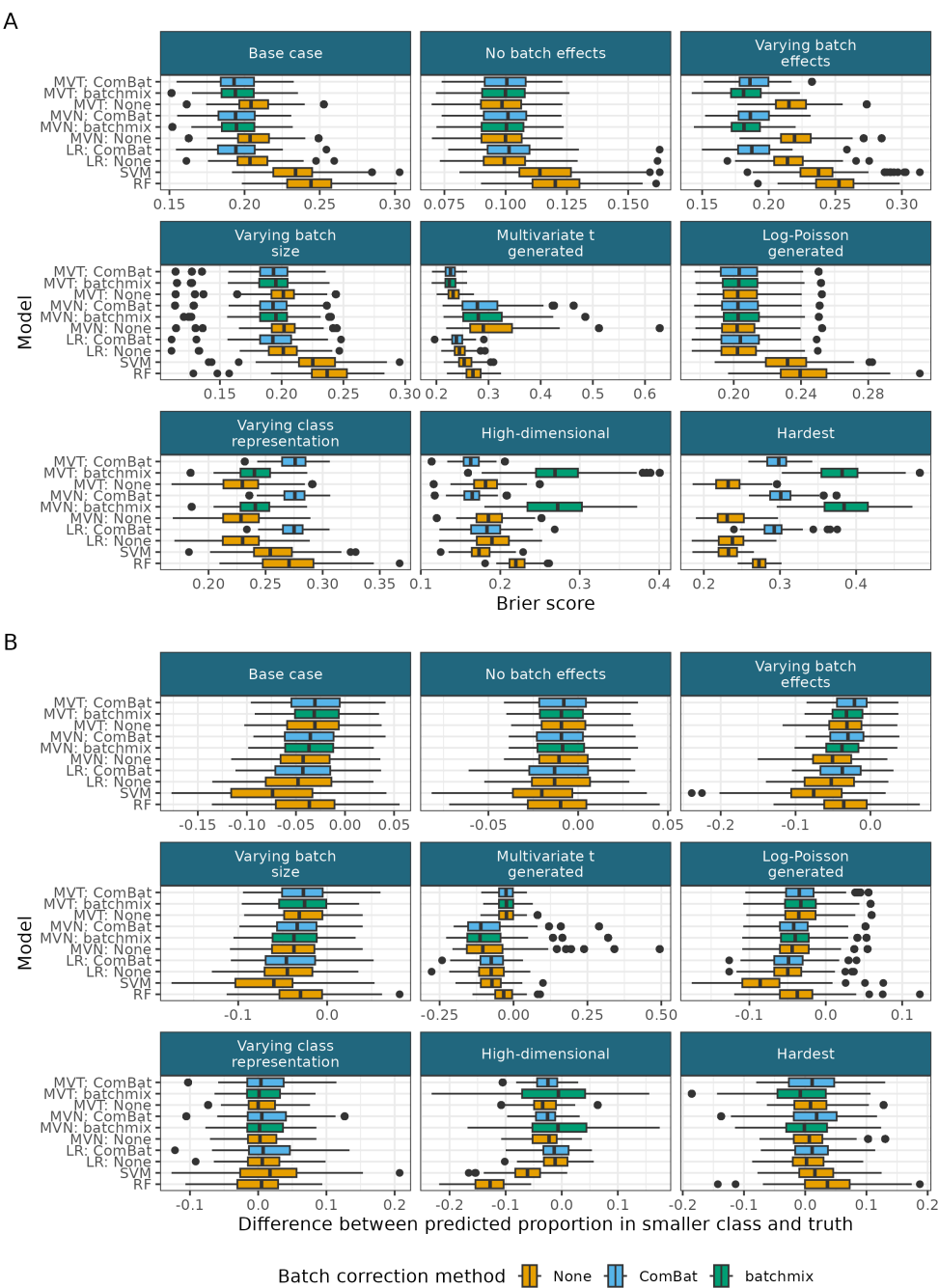


Figure 1: A) Brier score for the inferred allocation probability in the unlabelled data across simulations. B) The difference between the inferred proportion in class 2 and the true proportion of the data in class 2.

A semi-supervised Bayesian mixture modelling approach for joint batch correction and classification

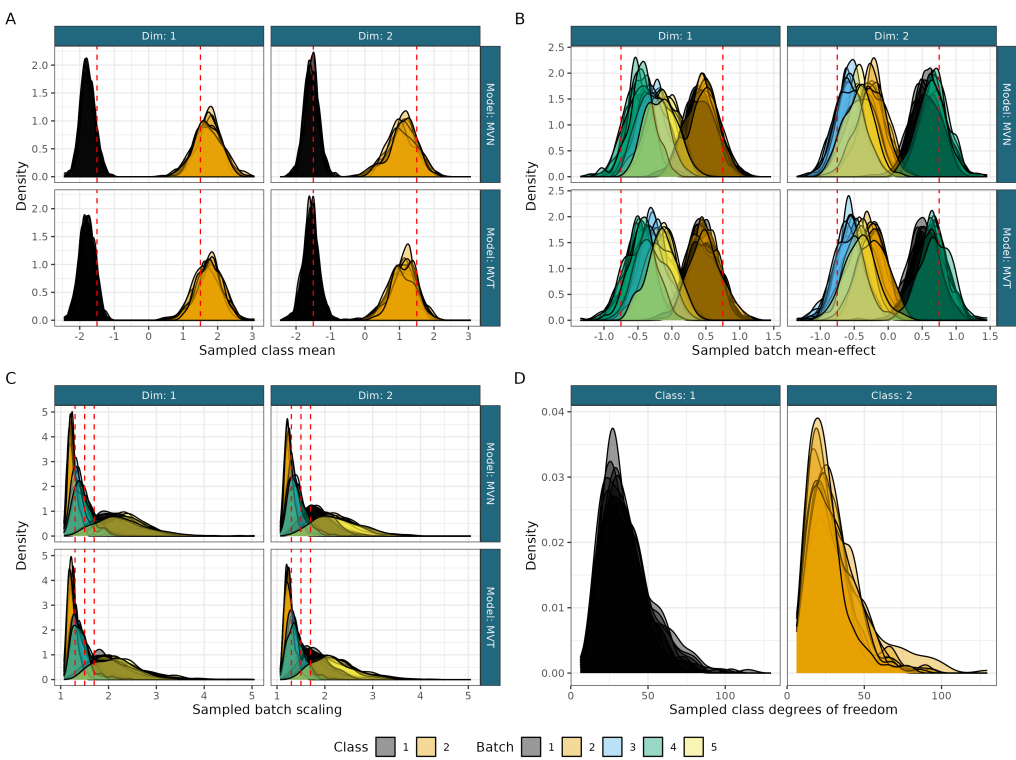


Figure 2: Sampled values for A) the class means, B) the batch mean-effect, C) the batch scaling effect and D) the class degrees of freedom for the well-behaved chains for the first simulated dataset in the Base case scenario. True values are shown by the dashed red vertical lines (as the data are generated from a MVN density there is no true degree of freedom, but larger values better approximate the MVN).

217 two scenarios a) the cell type and class are independent and b) the cell type and batch are correlated (figure
 218 3 A and B; the generating models are described in section 5 of the supplementary material). We consider
 219 the same set of models as in the simulation study and aim to infer cell type for the data with hidden labels.
 220 We hide a random 80% of labels in each of ten folds with the restriction that each class has at least one
 221 known member. We compare model performance using the Brier score. The results are similar to the Base
 222 case scenario in the simulation study with the semi-supervised Bayesian mixture models performing the
 223 best. When there is no dependency between class and batch ComBat and batchmix are equivalent, but when
 224 this dependency is present ComBat suffers significantly. In this case doing no batch correction is the best
 225 strategy, followed closely by batchmix. In both scenarios the off-the-shelf supervised methods perform less
 226 well than the semi-supervised mixture models.

A semi-supervised Bayesian mixture modelling approach for joint batch correction and classification

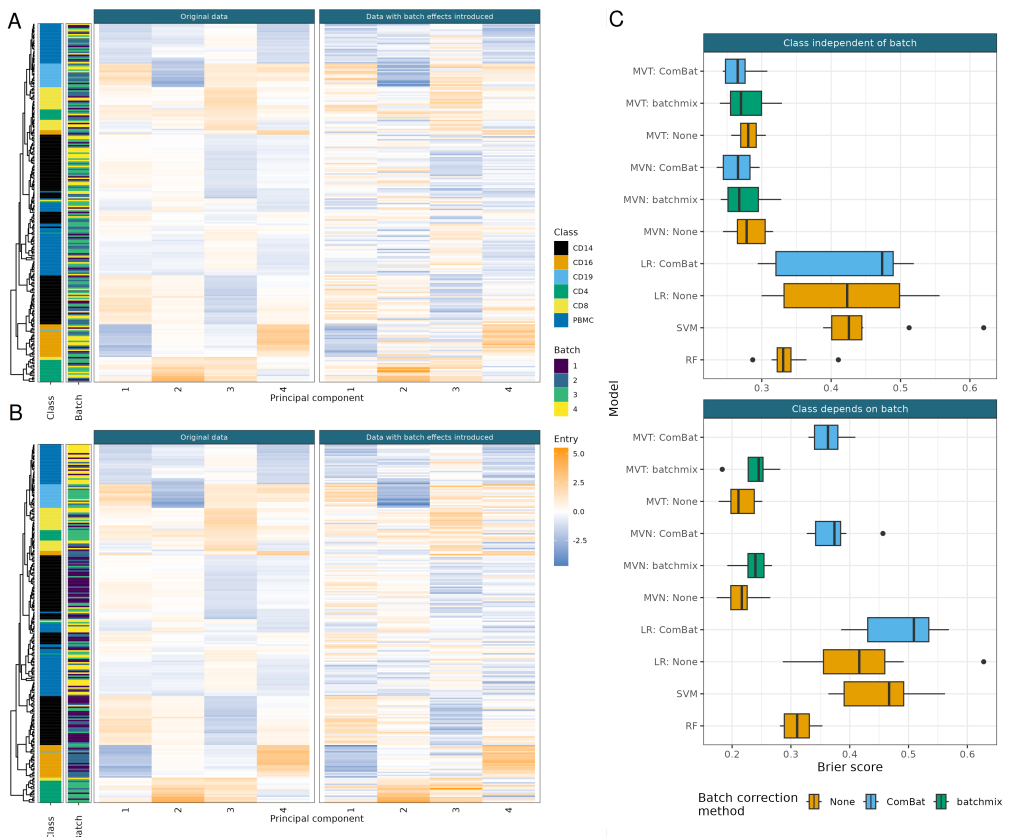


Figure 3: The data and model performance for the cell gene expression data. A) Facet on the left shows the original data, annotated by class and batch. The facet on the right shows the data after batch effects are introduced for class independent of batch. B) As A) but class is dependent on batch. C) Model performance across 10 folds under the Brier score for both scenarios.

227 5 ELISA data examples

228 ELISA is an immunological assay used to measure antibodies, antigens, proteins and glycoproteins, and
 229 normally involves a reaction that converts the substrate into a coloured product, the optical density (**OD**)
 230 which can be measured and is then used to determine the antigen concentration. One application is to assess
 231 seroprevalence of a disease within a population by measuring seropositivity of antibodies. It has a history of
 232 application to a wide range of diseases (e.g., 38, 3, 17, 30) and was used extensively to study seropositivity
 233 of antibodies to SARS-CoV-2 antigens used to estimate prevalence of cumulative infection and immunity
 234 (12, 29, 37). In such cases it is often possible to include known positive and negative controls as samples
 235 (these might be PCR-positive patients and historical samples collected before the pandemic began) and thus
 236 a subset of labels are observed.

A semi-supervised Bayesian mixture modelling approach for joint batch correction and classification

237 We investigated the performance of our model on two recent examples of ELISA data, both from studies
238 estimating seroprevalence of SARS-CoV-2. Based on the results from the simulations, we use the MVT as
239 our choice of density, as it always matched or outperformed the MVN mixture in simulations (figure 1).

240 In the ELISA datasets we do not know the true seropositive status for the non-control data and cannot
241 evaluate the model accuracy. Rather, we present these to demonstrate application of our model and highlight
242 how diagnostic plots and results may be interpreted. In each case we run multiple chains and then use the
243 sampled log-likelihood to assess within and across chain convergence.

244 Traditional analysis of ELISA data in seroprevalence studies makes dichotomous calls according to thresh-
245 olds based on the sum of the sample mean and some number of standard deviations of the negative controls
246 in each measurement. However, various choices of the number of standard deviations to use to define the
247 decision boundary are present in the literature (e.g., compare 12, 29, 37).

248 5.1 Carlos Dopico *et al.*, 2021

249 We used the dataset available from Castro Dopico *et al.* (7), with the *group* variable representing the batch
250 divisions. This dataset comprises the log-transformed normalised OD for IgG responses against stabilized
251 trimers of the SARS-CoV-2 spike glycoprotein (SPIKE) and the smaller receptor-binding domain (RBD)
252 in 2,100 sera samples from blood donors, 2,000 samples from pregnant volunteers, 595 historical negative
253 controls, repeatedly sampled, and 149 PCR-positive patients (positive controls from 8). The data were
254 generated across seven batches, with the positive controls contained in two of these. This, combined with our
255 expectation that seropositivity should increase with time as more of the population were exposed to SARS-
256 CoV-2, suggests that the batch and seropositivity frequency are dependent. Based on our simulation study,
257 we would expect that a pre-processing batch normalisation would therefore produce misleading results.

258 We ran five chains of the MVT mixture model for 50,000 iterations for each of nine combinations of different
259 choices for the hyperparameters of the batch effects in the model (choices in table 1, distributions in figure
260 4 A and B). The first 20,000 samples were removed as burn-in, and we thinned to every 100th sample to
261 reduce auto-correlation.

	Value								
α	1	5	10	1	5	10	1	5	10
β	3	11	21	3	11	21	3	11	21
λ	0.01	0.01	0.01	0.10	0.10	0.10	1.00	1.00	1.00

Table 1: Hyperparameter combinations used in analysing the data from Castro Dopico *et al.* (7). The prior expected value of the batch scaling effect is the same for all choices of α and β . The choice of λ represents the scale we *a priori* expect for the batch shift effect.

A semi-supervised Bayesian mixture modelling approach for joint batch correction and classification

262 We chose a representative chain for each hyperparameter combination to estimate the seroprevalence for
263 each week of the year 2020 for which samples are available and compared these to the estimates from
264 Castro Dopico et al. (7) (figure 4 C). Our point estimate was the mean posterior probability of allocation for
265 the non-control data. This was highly consistent across hyperparameter choices and was contained within
266 the confidence interval of the estimate provided by Castro Dopico et al. (7). However, our seroprevalence
267 point estimates, particularly in later dates, were higher than the those from Castro Dopico et al. (7). Table 1
268 of the Supplementary material shows the point estimate from the ML methods used in the Simulation study,
269 our MVT mixture model and that from the original paper. This shows that while our method provides higher
270 point estimates than those from Castro Dopico et al. (7), the other ML methods (barring the SVM) provide
271 estimates much closer to or even exceeding that from the MVT.

272 The seroprevalence estimates and their credible intervals were almost identical across hyperparameter
273 choices, suggesting that the classification results are robust to different choices for these hyperparame-
274 ters. We took a single chain with hyperparameter choice $\alpha = 5, \beta = 11$ and $\lambda = 0.1$ as a representative
275 example. This value of λ represents our expectation that m_b should be approximately an order of magnitude
276 smaller than μ_k . We used this to infer a point classification and a batch-corrected dataset (figure 5). Note
277 that the data were on a similar scale to the observed data (figure 5), the lack of identifiability for parameters
278 in the likelihood function did not emerge as a problem here. The batch-corrected dataset was better visually
279 separated into seronegative and seropositive classes than the observed data due to our batch-correction.

280 To confirm the batch-correction was working as intended we considered repeated control samples from a
281 particular patient, “Patient 4”, and the negative controls in batches with a high proportion of negative controls
282 (> 100). The Patient 4 samples were all collected at the same time and were included in several plates as a
283 positive control but discarded before our analysis because it was chosen for extremely high antibody levels
284 and so is unrepresentative, even for the seropositive class. We hypothesised that appropriate batch-correction
285 should bring the different measurements of this sample closer together, which is indeed what we observed
286 after applying the correction learnt from the samples excluding Patient 4 (figure 6 A). Before correction,
287 the batches had no overlap; there was a distance of 0.197 between the batch means. After correction the
288 two batches overlapped with a distance of 0.040 between the means as the points moved closer together
289 and towards the class mean (figure 6 A would correspond to the upper right hand of figure 5). For the set
290 of negative controls we consider, we expected that these batches should have overlap more after correction
291 as their relationship between batch and class should be similar. This is what we observed (figure 6 B) and
292 the variance explained in the SPIKE and RBD optical density by the batch variable for these samples is
293 significantly lower after the batch-correction. For SPIKE OD, 4.2% of the variation is explained by batch of

A semi-supervised Bayesian mixture modelling approach for joint batch correction and classification

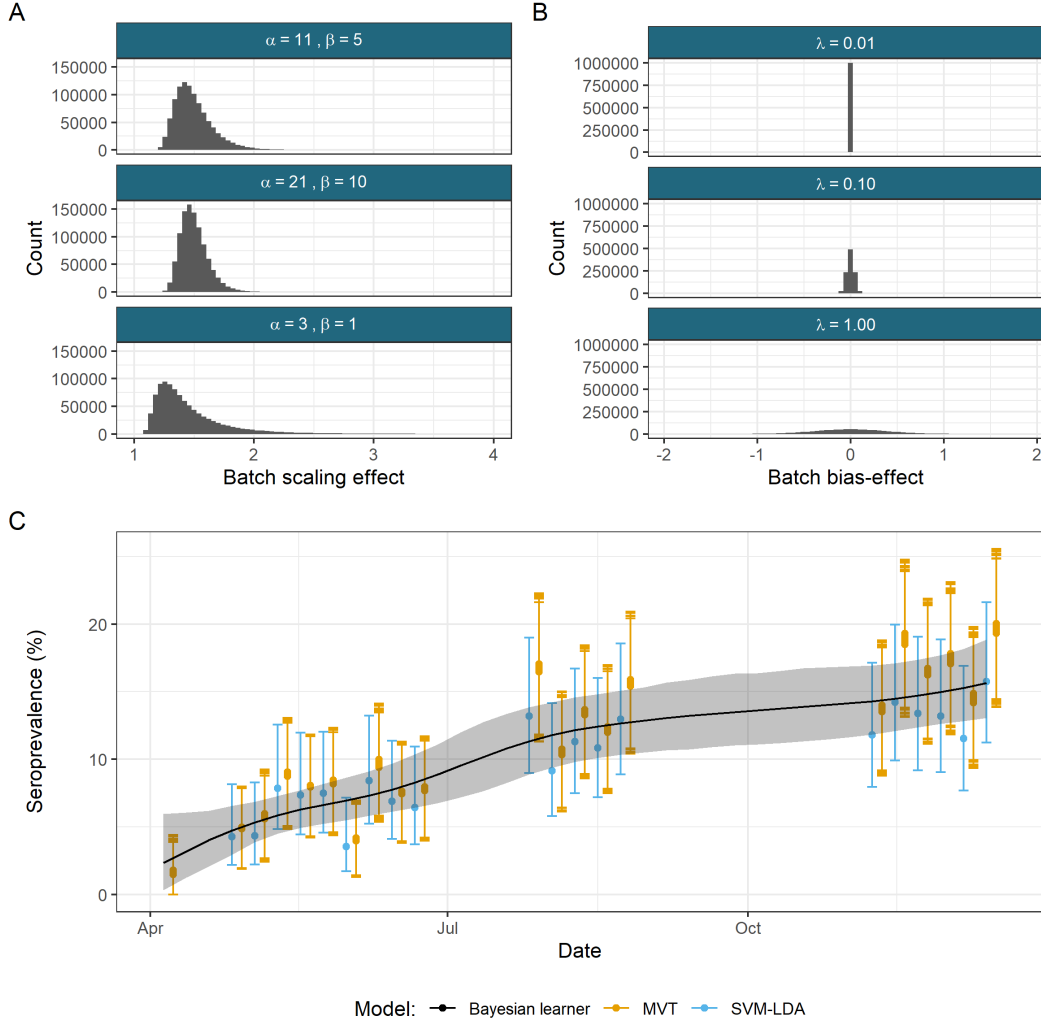


Figure 4: Effect of hyperparameter choices on seroprevalence estimates. One million draws from the prior distributions for the different hyperparameter choices for A) the batch scaling effect and B) the batch shift effect. In A) draws exceeding a value of 4 are hidden. This means that approximately 0.5% of the draws from the prior distribution with a shape of 3 and a scale of 1 are not shown. C) A comparison of the estimated seroprevalence with population 95% confidence intervals for the MVT mixture model with nine different choices of hyperparameters for the batch-effect prior distributions and the estimates from Castro Dopico et al. (7) for the SVM-LDA ensemble model and the Bayesian learner from Christian and Murrell (9). The Bayesian learner is designed to estimate seroprevalence during an epidemic and provides a smooth, non-decreasing estimate across time. Its assumptions ensure a more consistent increase across time, whereas the SVM-LDA and MVT mixture models are not incorporating any explicit temporal information. The estimates from the mixture model have been moved 3 days to the right on the x -axis to reduce overlap.

A semi-supervised Bayesian mixture modelling approach for joint batch correction and classification

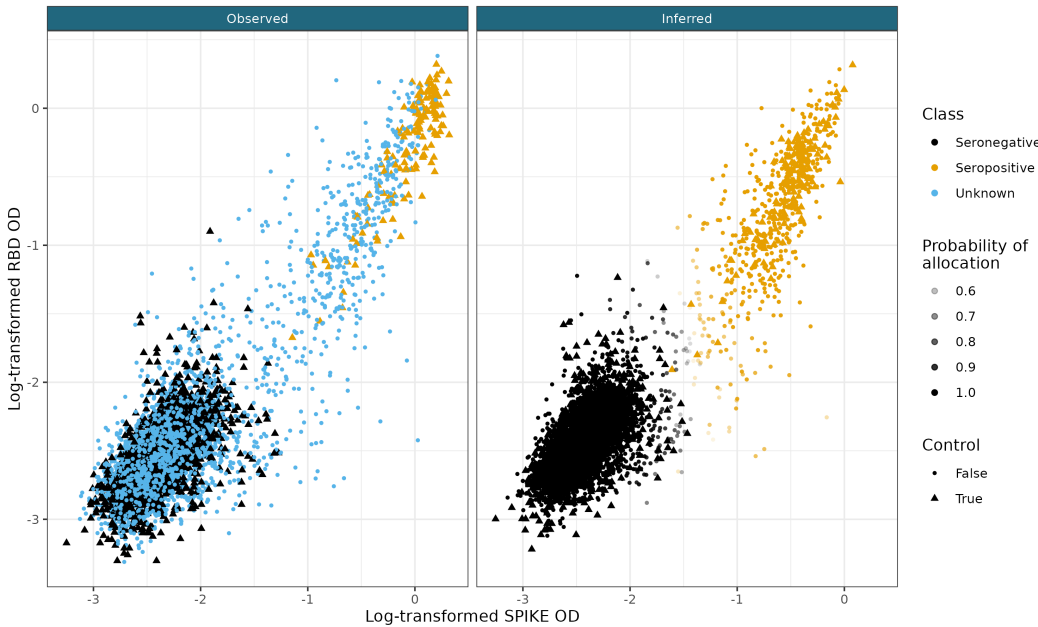


Figure 5: In the first facet, the observed data from Castro Dopico et al. (7) and on the right, the point estimate of the inferred, batch-corrected dataset from the MVT mixture model with $\alpha = 11$, $\beta = 5$, $\lambda = 0.1$. Points on both plots are coloured by the class. In the observed dataset non-control points are labelled “Unknown” and in the batch-corrected dataset these points are labelled with their inferred class and have their opacity controlled by the inferred allocation probability.

294 origin in the observed data, 0.5% is explained in the batch-corrected data. For the RBD optical density, the
 295 respective figures are 4.3% and 1.4%.

296 5.2 Pseudo-ELISA data

297 We wished to investigate the possibility that other known positive samples could be more extreme than the
 298 non-hospitalised donors. To examine this, we generated datasets from the model fitted in section 5.1. This
 299 also tests if the model has learnt representative parameters for the dataset, as our generated data should be
 300 very similar to the original data. We used the MCMC sample mean for each parameter except the class
 301 weights. For the class weights we used the inferred proportion of each class in each batch to preserve the
 302 problem of the imbalance of classes across batches. In the original data, the positive controls were more
 303 extreme members of the positive class, having sufficiently severe symptoms to have undergone PCR testing
 304 when such resources were severely constrained early in the pandemic. To reflect this in our data generation
 305 procedure, we increased the probability that samples with observed positive labels (i.e., the positive controls)
 306 are from the tail of the distribution of the seropositive measurements which is furthest from the seronegative
 307 class, whereas the negative controls are sampled uniformly from the seronegative population. An example
 308 dataset is shown in figure 7 C, note how closely it resembles the true ELISA data in figure 5, suggesting that

A semi-supervised Bayesian mixture modelling approach for joint batch correction and classification

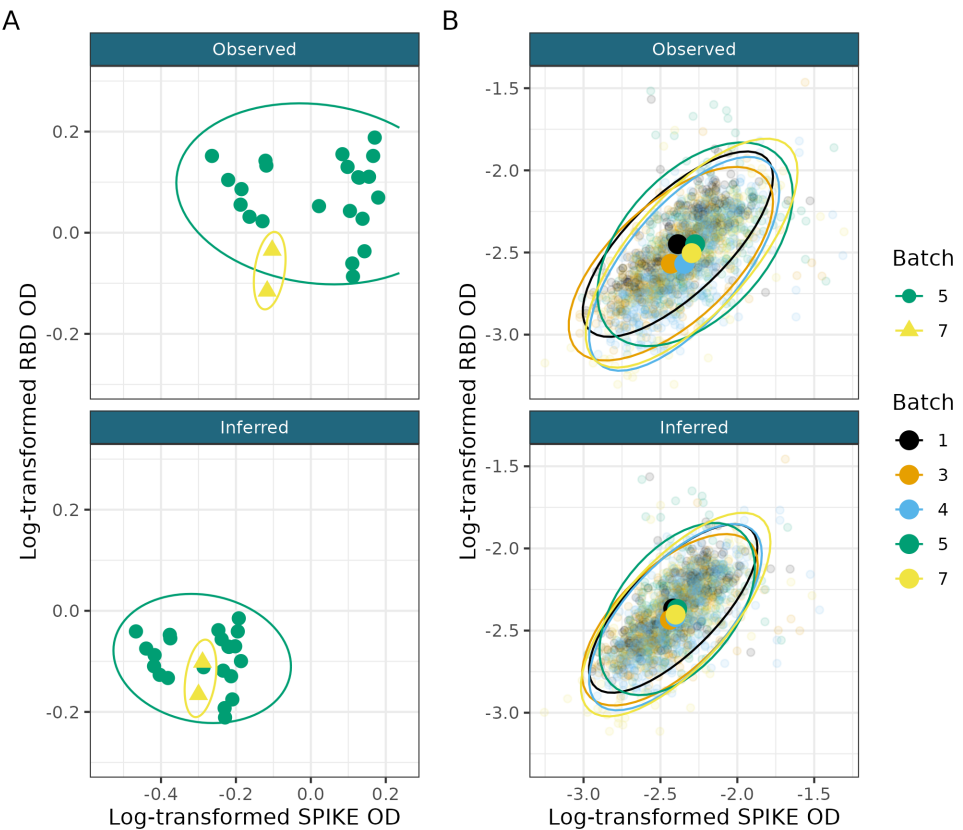


Figure 6: A) The samples from Patient 4 as observed and after batch correction. B) The mean and covariance for the batches containing a large number (> 100) seronegative controls as observed and after batch-correction. Note that the means overlap significantly more and relationship between SPIKE and RBD is more uniform across batches after the correction.

309 the model has learnt accurate values. See section 8 of the supplementary material for a deeper explanation
310 of the generation process.

311 We performed a similar analysis to our original simulation study on these datasets, comparing our models to
312 a range of off-the-shelf machine learning methods. Across all of the simulations, we found that our mixture
313 models outperformed other methods under both the F1 score and the squared distance (figures 7 A, 7 B).
314 The semi-supervised Bayesian mixture model also performed well here; this is due to the large proportion
315 of negative samples in a single batch and the large imbalance in class sizes (approximately 19 to 1).

316 5.3 Dingens et al., 2020

317 As a final real data example, we analysed the ELISA data collected by Dingens et al. (12). This consisted
318 of 1,891 measurements of antibodies to the SARS-CoV-2 RBD protein. 1,783 of these were from residual
319 serum from Seattle Children's Hospital, with 52 pre-2020 samples used as negative controls and 52 samples

A semi-supervised Bayesian mixture modelling approach for joint batch correction and classification

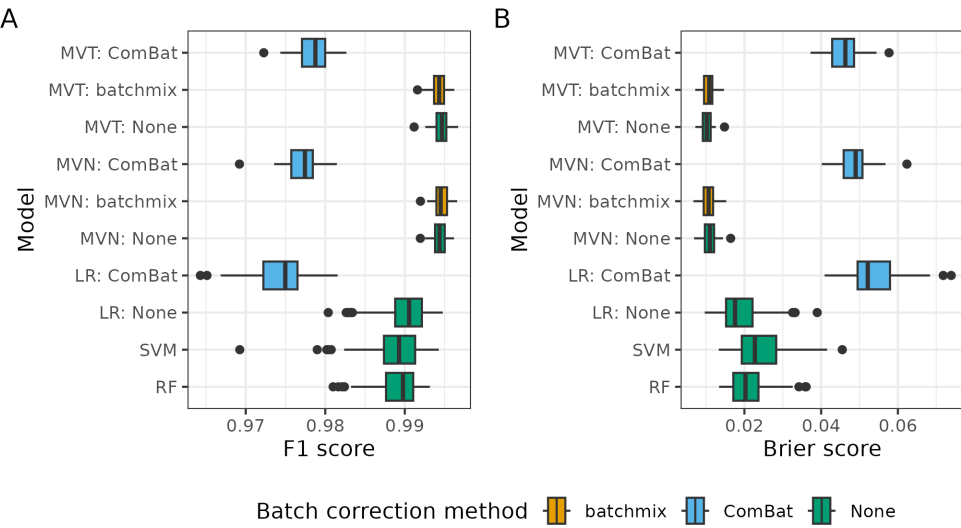


Figure 7: Performance of different methods across 100 datasets simulated from the converged MVT model for the ELISA data from Castro Dopico et al. under A) the F1 score and B) the Brier score.

320 from individuals with RT-PCR-confirmed infections as positive controls (figure 8 A). These data are different
 321 to the data from Castro Dopico et al. (7) in several ways. There is only a single antigen, there is a smaller
 322 ratio of controls to non-controls, particularly for the seronegative samples, and the controls do not appear
 323 to be representative of either class. The mean log OD of the negative controls is -1.91, whilst the dataset
 324 mean is -2.28 without controls. We analyse the log-transform of the OD using our MVT model for the
 325 same variety range of hyperparameter choices as in table 1. An example of a batch-corrected dataset is
 326 shown in figure 8 B. We show the comparison of the inferred seroprevalence in each batch for an example
 327 chain of each of these models as well as that estimated by Dingens et al. (12) (figure 8 C). The 9 different
 328 hyperparameter choices have almost identical seroprevalence estimates and are estimating higher levels of
 329 seroprevalence than the estimate provided by Dingens et al. (12).

330 6 Discussion

331 The results of our simulation study show that our mixture model consistently matches or outperforms several
 332 alternatives when applied to data with batch effects, across a range of data generating models. We believe
 333 that the simulation study and the gene expression analysis shows our method is a good model choice in a low-
 334 dimensional setting. If batch and class are independent, it performs almost identically to ComBat, but it is
 335 much stronger when this dependency exists. On the other side of the spectrum, using the standalone mixture
 336 model with no batch-correction is also a viable option, but when batch effects are large (as in the Varying

A semi-supervised Bayesian mixture modelling approach for joint batch correction and classification

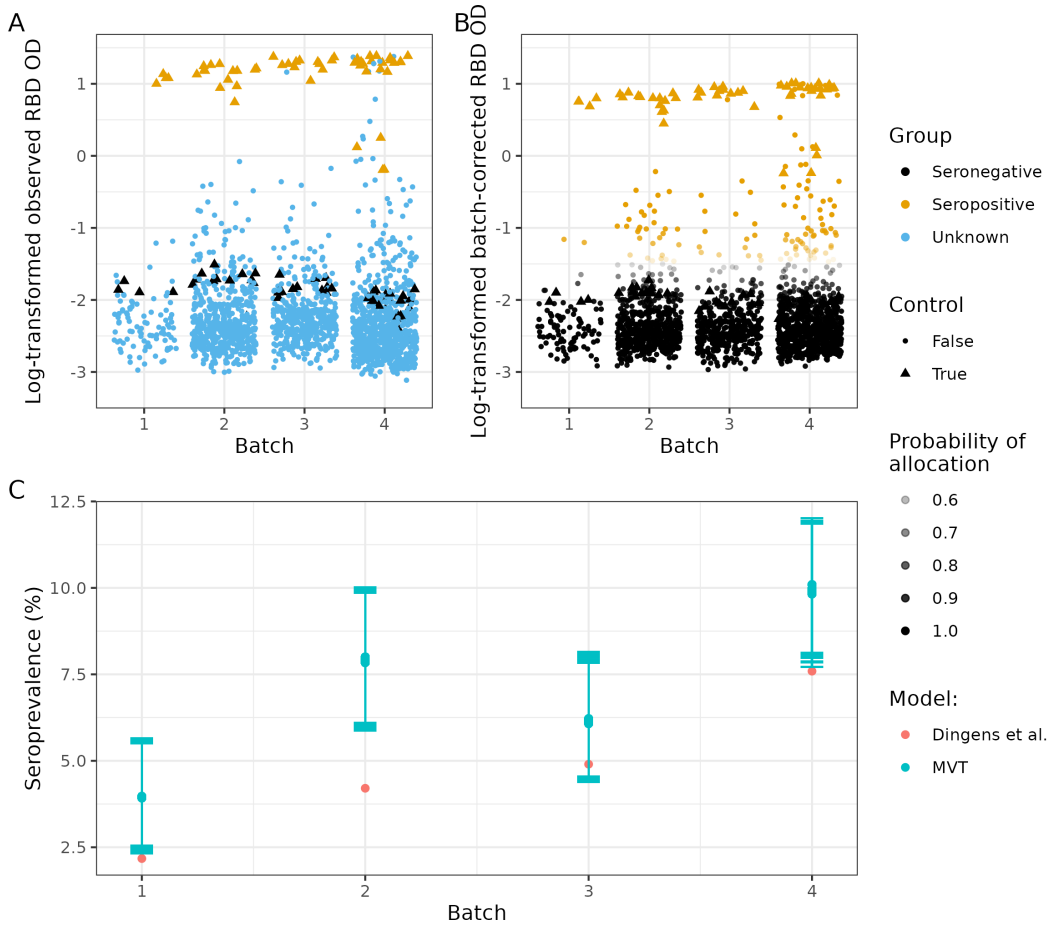


Figure 8: A) The observed data from Dingens et al. (12) and B) the point estimate of the batch-corrected dataset from the MVT mixture model with $\alpha = 11$, $\beta = 5$, $\lambda = 0.1$. Points on both plots are coloured by the class. In the observed dataset non-control points are labelled “Unknown” and in the batch-corrected dataset these points are labelled with their inferred class. C) A comparison of the seroprevalence estimate from the MVT mixture model with nine different choices of batch-effect hyperparameters and that from Dingens et al. (12). The error bars indicate the 95% credible interval for the seroprevalence estimates of the MVT mixture model in each batch; this is not available for the estimate from Dingens et al. (12).

337 batch effects scenario), this is significantly worse than including a batch correction. As the relationship
 338 between batch and class and the magnitude of the batch effects is rarely known, we believe our model offers
 339 a better guarantee of meaningful inference. In the more specific scenario where data were generated from
 340 a converged chain that had been applied to the ELISA data from Castro Dopico et al. (7), we obtained the
 341 same findings, with our model again performing better than the off-the-shelf machine learning methods and
 342 ComBat over-correcting for batch due to the imbalance of classes. We also see from our simulation study
 343 that we should use the MVT density over the MVN density, as the MVT can approximate the MVN quite
 344 well by learning a large degree of freedom, but also has additional flexibility as shown by the Multivariate
 345 t generated simulation scenario where the MVN mixture model behaved very inconsistently. The only cost

A semi-supervised Bayesian mixture modelling approach for joint batch correction and classification

346 of the MVT mixture model is the approximate 50% increase in runtime, but as our implementation is quite
347 fast we believe that this is not a significant detractor. Based on these results we recommend the use of our
348 MVT mixture model when the analyst suspects the classes in the data may be non-Gaussian.

349 In terms of estimating seroprevalence, our mixture model performed very well in our simulation study.
350 Using the results shown in figure 1 B, we can try to gauge how well our method is performing in the ELISA
351 data. We would argue that the most pertinent scenarios are the MVT generated (the ELISA data are non-
352 Gaussian), the Varying batch effects and the Varying class representation scenarios. Our method estimates
353 seroprevalence close to the truth, or slightly smaller, in these simulations. Based on this, we suspect that the
354 high estimates of seroprevalence provided by our model (relative to those from the original papers) in the
355 ELISA analyses are plausible.

356 In the Swedish dataset, we are reassured that the batch-correction is reasonable by our analysis of the patient
357 4 samples - these samples were used across several batches as positive controls; after applying the correction
358 learnt on the dataset excluding these extreme samples they are no longer separable by batch and have moved
359 towards the class mean. The data generated from our converged model also appears very similar to the
360 observed data, suggesting that the model assumptions are reasonable, and that meaningful estimates of the
361 parameters were obtained.

362 In the analysis using the data from Dingens et al. (12), the unrepresentative negative controls presented a
363 problem. We believe that the preceding analyses show the potential advantages of our model over existing
364 methods, but this dataset is a good example to show that our method is not a panacea that may overcome all
365 problems - it remains vital to have useful and relevant data in order to perform meaningful inference (13).
366 Any analysis that uses training data that appear to be drawn from a different population than the test data
367 is unlikely to produce meaningful results. Furthermore, the data are not well-described by a pair of MVT
368 distributions (even allowing for our additional flexibility with the batch parameters). This combination of
369 model misspecification and misleading training data makes us skeptical of the inferred parameters.

370 We note, however, that in the simulation of pseudo-ELISA data, our method still performed strongly despite
371 the positive controls not being representative of the general seropositive sample. In this case our model was
372 correctly specified (the data are generated from a MVT mixture model). In general, we suspect that our
373 method is useful if either the assumption that the labelled data represent their class well or that the model
374 density choice is correct are slightly relaxed, but if both do not hold or if either is profoundly wrong then
375 the model will perform poorly.

A semi-supervised Bayesian mixture modelling approach for joint batch correction and classification

376 Since only the combined class and batch parameters, $\mu_k + m_b$ and $\Sigma_k \oplus S_b$, are identifiable, one might
377 expect this to present challenges when fitting our model. However, Redner (35) showed that the maximum-
378 likelihood estimator is consistent when the distributions are not identifiable and the nonuniqueness is caused
379 by the particular parameterization. Note that even if the individual batch and class parameters never stabilise
380 (note that their combinations are identifiable and should converge), running multiple chains helps to avoid
381 this potential pitfall as one could use the trace plots for the complete likelihood to assess if the chains have
382 reached a common mode in the likelihood surface even if the individual batch and class parameters did not
383 converge. This is standard practice when using stochastic methods, so this aspect of the model should not
384 introduce additional work to the recommended Bayesian workflow (15). Furthermore, from the similarity
385 of the inferred parameters across multiple chains in the Base case simulation (figure 2), we have empirical
386 evidence that this behaviour is not common. We also saw that the seroprevalence estimates and their credible
387 intervals across different hyperparameter choices in the ELISA analyses were well-behaved and, as a result,
388 so was the inferred allocation. This similarity across hyperparameter choice suggests that choosing between
389 specific values is not too important, but we suspect that, if the sample size is smaller, having λ close to
390 one could exacerbate the identifiability problem for the batch shift effect and the class mean. Therefore, we
391 suggest setting $\lambda \leq 0.1$ to encourage these parameters to converge in the small sample setting (although
392 note that their sum, $\mu_k + m_b$, should converge regardless).

393 We have developed a Bayesian method to predict class membership and perform batch-correction simulta-
394 neously, developing on the pre-processing, univariate method of Johnson et al. (19). Our method is intended
395 for low-dimensional data, but the main limitation for higher dimensional data is computational (inverting
396 the covariance matrix becomes very costly) rather than theoretical. Our model is not strictly limited to the
397 semi-supervised setting either; it could be used for unsupervised learning. In this case we expect that the
398 model will rely much more heavily on the distributional assumptions. Our work could be extended to include
399 alternative densities, such as the skew multivariate t . We could extend the model to include batch-specific
400 class weights, such as we used to generate the data in our Varying class representation simulation scenario,
401 or a deeper hierarchy for the batch parameters, such as nested batches (e.g., this could represent scenarios
402 where multiple plates are run at each of multiple time points or locations).

403 Funding

404 This work was funded by the Medical Research Council (MC UU 00002/4, MC UU 00002/13) and the
405 Wellcome Trust (WT2200788, WT220024) and supported by the NIHR Cambridge Biomedical Research
406 Centre (BRC-1215-20014). The views expressed are those of the author(s) and not necessarily those of the

A semi-supervised Bayesian mixture modelling approach for joint batch correction and classification

407 NHS, the NIHR or the Department of Health and Social Care. For the purpose of Open Access, the author
408 has applied a CC BY public copyright licence to any Author Accepted Manuscript version arising from this
409 submission.

410 Competing interests

411 CW receives research funding from GSK and MSD for an unrelated project and is a part-time employee of
412 GSK. These companies had no input into this study.

413 Acknowledgements

414 We would like to thank Dingens et al. (12), specifically Janet A. Englund and Jesse D. Bloom, for being
415 willing to openly share their data and batch information.

416 Authors' contributions

417 SC, PK and CW all contributed to model design. SC implemented the model in C++ and built the R package
418 with PK and CW contributing to debugging strategies. SC designed the simulation study and the pseudo-
419 ELISA data. SC, PK and CW all contributed to the design of the Metropolis algorithm used to implement the
420 model and the choice of proposal densities. PK, CW and SC all contributed to analysis and the interpretation
421 of results. KN wrangled and cleaned the gene expression data. XD and GK generated the first ELISA dataset
422 which CW cleaned. All authors read and approved the manuscript.

423 References

424 [1] Emanuele Aliverti, Kristian Lum, James E. Johndrow, and David B. Dunson. Removing the influence
425 of group variables in high-dimensional predictive modelling. *Journal of the Royal Statistical Society: Series A (Statistics in Society)*, 184(3):791–811, 2021. ISSN 1467-985X. doi: 10.1111/rssa.12613.

426

427 [2] O. Alter, P. O. Brown, and D. Botstein. Singular value decomposition for genome-wide expression data
428 processing and modeling. *Proceedings of the National Academy of Sciences*, 97(18):10101–10106,
429 August 2000. ISSN 0027-8424, 1091-6490. doi: 10.1073/pnas.97.18.10101.

430

431 [3] Stuart D. Blacksell, Richard G. Jarman, Robert V. Gibbons, Ampai Tanganuchitcharnchai, Mammen P.
432 Mammen, Ananda Nisalak, Siripen Kalayanaroj, Mark S. Bailey, Ranjan Premaratna, H. Janaka de Silva, Nicholas P. J. Day, and David G. Lalloo. Comparison of Seven Commercial Antigen and

A semi-supervised Bayesian mixture modelling approach for joint batch correction and classification

433 Antibody Enzyme-Linked Immunosorbent Assays for Detection of Acute Dengue Infection. *Clinical*
434 and *Vaccine Immunology*, 19(5):804–810, May 2012. ISSN 1556-6811, 1556-679X. doi: 10.1128/
435 CVI.05717-11.

436 [4] Bernhard E. Boser, Isabelle M. Guyon, and Vladimir N. Vapnik. A training algorithm for optimal
437 margin classifiers. In *Proceedings of the Fifth Annual Workshop on Computational Learning Theory*,
438 COLT '92, pages 144–152, New York, NY, USA, July 1992. Association for Computing Machinery.
439 ISBN 978-0-89791-497-0. doi: 10.1145/130385.130401.

440 [5] Leo Breiman. Random Forests. *Machine Learning*, 45(1):5–32, October 2001. ISSN 1573-0565. doi:
441 10.1023/A:1010933404324.

442 [6] Andrew Butler, Paul Hoffman, Peter Smibert, Efthymia Papalex, and Rahul Satija. Integrating single-
443 cell transcriptomic data across different conditions, technologies, and species. *Nature Biotechnology*,
444 36(5):411–420, May 2018. ISSN 1546-1696. doi: 10.1038/nbt.4096.

445 [7] X. Castro Dopico, S. Muschiol, M. Christian, L. Hanke, D. J. Sheward, N. F. Grinberg, J. Rorbach,
446 G. Bogdanovic, G. M. Mcinerney, T. Allander, C. Wallace, B. Murrell, J. Albert, and G. B. Karlsson
447 Hedestam. Seropositivity in blood donors and pregnant women during the first year of SARS-CoV-2
448 transmission in Stockholm, Sweden. *Journal of Internal Medicine*, May 2021. ISSN 1365-2796. doi:
449 10.1111/joim.13304.

450 [8] Xaqin Castro Dopico, Leo Hanke, Daniel J. Sheward, Sandra Muschiol, Soo Aleman, Nas-
451 tasiya F. Grinberg, Monika Adori, Murray Christian, Laura Perez Vidakovics, Changil Kim, Sharesta
452 Khoenkhoen, Pradeepa Pushparaj, Ainhoa Moliner Morro, Marco Mandolesi, Marcus Ahl, Mattias
453 Forsell, Jonathan Coquet, Martin Corcoran, Joanna Rorbach, Joakim Dillner, Gordana Bogdanovic,
454 Gerald M. McInerney, Tobias Allander, Ben Murrell, Chris Wallace, Jan Albert, and Gunilla B. Karls-
455 son Hedestam. Probabilistic approaches for classifying highly variable anti-sars-cov-2 antibody re-
456 sponses. *medRxiv*, 2021. doi: 10.1101/2020.07.17.20155937. URL <https://www.medrxiv.org/content/early/2021/01/06/2020.07.17.20155937>.

457

458 [9] Murray Christian and Ben Murrell. Discriminative Bayesian Serology: Counting Without Cutoffs.
459 *bioRxiv*, 2020. doi: 10.1101/2020.07.14.202150. URL <https://www.biorxiv.org/content/early/2020/07/14/2020.07.14.202150>.

460

461 [10] Oliver M. Crook, Claire M. Mulvey, Paul D. W. Kirk, Kathryn S. Lilley, and Laurent Gatto. A Bayesian
462 mixture modelling approach for spatial proteomics. *PLOS Computational Biology*, 14(11):e1006516,
463 November 2018. ISSN 1553-7358. doi: 10.1371/journal.pcbi.1006516.

A semi-supervised Bayesian mixture modelling approach for joint batch correction and classification

464 [11] Oliver M. Crook, Kathryn S. Lilley, Laurent Gatto, and Paul D. W. Kirk. Semi-supervised nonpara-
465 metric Bayesian modelling of spatial proteomics. *The Annals of Applied Statistics*, 16(4):2554 – 2576,
466 2022. doi: 10.1214/22-AOAS1603. URL <https://doi.org/10.1214/22-AOAS1603>.

467 [12] Adam S. Dingens, Katharine H. D. Crawford, Amanda Adler, Sarah L. Steele, Kirsten Lacombe,
468 Rachel Eguia, Fatima Amanat, Alexandra C. Walls, Caitlin R. Wolf, Michael Murphy, Deleah Pettie,
469 Lauren Carter, Xuan Qin, Neil P. King, David Veesler, Florian Krammer, Jane A. Dickerson, Helen Y.
470 Chu, Janet A. Englund, and Jesse D. Bloom. Serological identification of SARS-CoV-2 infections
471 among children visiting a hospital during the initial Seattle outbreak. *Nature Communications*, 11(1):
472 4378, September 2020. ISSN 2041-1723. doi: 10.1038/s41467-020-18178-1.

473 [13] David B. Dunson. Statistics in the Big Data era: Failures of the machine. *Statistics & Probability
474 Letters*, 136:4–9, 2018.

475 [14] Chris Fraley and Adrian E Raftery. Bayesian Regularization for Normal Mixture Estimation and
476 Model-Based Clustering. *Journal of classification*, page 27, 2007.

477 [15] Andrew Gelman, Aki Vehtari, Daniel Simpson, Charles C. Margossian, Bob Carpenter, Yuling Yao,
478 Lauren Kennedy, Jonah Gabry, Paul-Christian Bürkner, and Martin Modrák. Bayesian Workflow.
479 *arXiv:2011.01808 [stat]*, November 2020.

480 [16] John Geweke et al. *Evaluating the Accuracy of Sampling-Based Approaches to the Calculation of
481 Posterior Moments*, volume 196. Federal Reserve Bank of Minneapolis, Research Department Min-
482 neapolis, MN, 1991.

483 [17] Dane Granger, Heather Hilgart, Lori Misner, Jaime Christensen, Sarah Bistodeau, Jennifer Palm,
484 Anna K. Strain, Marja Konstantinovski, Dakai Liu, and Anthony Tran. Serologic testing for Zika
485 virus: Comparison of three Zika virus IgM-screening enzyme-linked immunosorbent assays and ini-
486 tial laboratory experiences. *Journal of clinical microbiology*, 55(7):2127–2136, 2017.

487 [18] Laleh Haghverdi, Aaron T. L. Lun, Michael D. Morgan, and John C. Marioni. Batch effects in single-
488 cell RNA sequencing data are corrected by matching mutual nearest neighbours. *Nature biotechnology*,
489 36(5):421–427, June 2018. ISSN 1087-0156. doi: 10.1038/nbt.4091.

490 [19] W. Evan Johnson, Cheng Li, and Ariel Rabinovic. Adjusting batch effects in microarray expression
491 data using empirical Bayes methods. *Biostatistics*, 8(1):118–127, January 2007. ISSN 1468-4357,
492 1465-4644. doi: 10.1093/biostatistics/kxj037.

A semi-supervised Bayesian mixture modelling approach for joint batch correction and classification

493 [20] Miguel A. Juárez and Mark F. J. Steel. Model-Based Clustering of Non-Gaussian Panel Data Based on
494 Skew- t Distributions. *Journal of Business & Economic Statistics*, 28(1):52–66, January 2010. ISSN
495 0735-0015, 1537-2707. doi: 10.1198/jbes.2009.07145.

496 [21] Alexandros Karatzoglou, Alex Smola, Kurt Hornik, and Achim Zeileis. kernlab – an S4 package
497 for kernel methods in R. *Journal of Statistical Software*, 11(9):1–20, 2004. URL <http://www.jstatsoft.org/v11/i09/>.

498 [22] Sharon X. Lee, Geoffrey J. McLachlan, and Saumyadipta Pyne. Modeling of inter-sample variation
499 in flow cytometric data with the joint clustering and matching procedure: Modeling of Inter-Sample
500 Variation. *Cytometry Part A*, 89(1):30–43, January 2016. ISSN 15524922. doi: 10.1002/cyto.a.22789.

501 [23] Jeffrey T. Leek, Robert B. Scharpf, Héctor Corrada Bravo, David Simcha, Benjamin Langmead,
502 W. Evan Johnson, Donald Geman, Keith Baggerly, and Rafael A. Irizarry. Tackling the widespread and
503 critical impact of batch effects in high-throughput data. *Nature Reviews. Genetics*, 11(10):733–739,
504 October 2010. ISSN 1471-0064. doi: 10.1038/nrg2825.

505 [24] Jeffrey T. Leek, W. Evan Johnson, Hilary S. Parker, Andrew E. Jaffe, and John D. Storey. The sva
506 package for removing batch effects and other unwanted variation in high-throughput experiments.
507 *Bioinformatics*, 28(6):882–883, 01 2012. ISSN 1367-4803. doi: 10.1093/bioinformatics/bts034. URL
508 <https://doi.org/10.1093/bioinformatics/bts034>.

509 [25] Tenglong Li, Yuqing Zhang, Prasad Patil, and W. Evan Johnson. Overcoming the impacts of two-step
510 batch effect correction on gene expression estimation and inference. *bioRxiv*, page 2021.01.24.428009,
511 January 2021. doi: 10.1101/2021.01.24.428009.

512 [26] Andy Liaw and Matthew Wiener. Classification and regression by randomforest. *R News*, 2(3):18–22,
513 2002. URL <https://CRAN.R-project.org/doc/Rnews/>.

514 [27] J Luo, M Schumacher, A Scherer, D Sanoudou, D Megherbi, T Davison, T Shi, W Tong, L Shi,
515 H Hong, C Zhao, F Elloumi, W Shi, R Thomas, S Lin, G Tillinghast, G Liu, Y Zhou, D Herman,
516 Y Li, Y Deng, H Fang, P Bushel, M Woods, and J Zhang. A comparison of batch effect removal
517 methods for enhancement of prediction performance using MAQC-II microarray gene expression data.
518 *The Pharmacogenomics Journal*, 10(4):278–291, August 2010. ISSN 1470-269X, 1473-1150. doi:
519 10.1038/tpj.2010.57.

520 [28] Paul Lyons, Eoin McKinney, Tim Rayner, Alexander Hatton, Hayley Woffendin, Maria Koukoulaki,
521 Thomas Freeman, David Jayne, Afzal Chaudhry, and Kenneth Smith. Transcription profiling of human

A semi-supervised Bayesian mixture modelling approach for joint batch correction and classification

523 separated leukocyte subsets in SLE and vasculitis. *BioStudies*, 2010. URL <https://www.ebi.ac.uk/biostudies/arrayexpress/studies/E-MTAB-145>.

524

525 [29] Reuben McGregor, Alana L. Whitcombe, Campbell R. Sheen, James M. Dickson, Catherine L. Day, Lauren H. Carlton, Prachi Sharma, J. Shaun Lott, Barbara Koch, Julie Bennett, Michael G. Baker, Stephen R. Ritchie, Shivani Fox-Lewis, Susan C. Morpeth, Susan L. Taylor, Sally A. Roberts, Rachel H. Webb, and Nicole J. Moreland. Collaborative networks enable the rapid establishment of serological assays for SARS-CoV-2 during nationwide lockdown in New Zealand. *PeerJ*, 8:e9863, 529 September 2020. ISSN 2167-8359. doi: 10.7717/peerj.9863.

530

531 [30] Caroline E. Mullis, Oliver Laeyendecker, Steven J. Reynolds, Ponsiano Ocama, Jeffrey Quinn, Iga Boaz, Ronald H. Gray, Gregory D. Kirk, David L. Thomas, and Thomas C. Quinn. High frequency 532 of false-positive hepatitis C virus enzyme-linked immunosorbent assay in Rakai, Uganda. *Clinical 533 infectious diseases*, 57(12):1747–1750, 2013.

534

535 [31] S. K. Ng, G. J. McLachlan, K. Wang, L. Ben-Tovim Jones, and S.-W. Ng. A Mixture model with 536 random-effects components for clustering correlated gene-expression profiles. *Bioinformatics*, 22(14): 537 1745–1752, July 2006. ISSN 1367-4803, 1460-2059. doi: 10.1093/bioinformatics/btl165.

538

539 [32] Vegard Nygaard, Einar Andreas Rødland, and Eivind Hovig. Methods that remove batch effects while 540 retaining group differences may lead to exaggerated confidence in downstream analyses. *Biostatistics (Oxford, England)*, 17(1):29–39, January 2016. ISSN 1465-4644. doi: 10.1093/biostatistics/kxv027.

541

542 [33] Sandhya Prabhakaran, Elham Azizi, Ambrose Carr, and Dana Pe'er. Dirichlet Process Mixture Model 543 for Correcting Technical Variation in Single-Cell Gene Expression Data. *International Conference on Machine Learning*, page 10, June 2016.

544

545 [34] R Core Team. *R: A Language and Environment for Statistical Computing*. R Foundation for Statistical Computing, Vienna, Austria, 2021. URL <https://www.R-project.org/>.

546

547 [35] Richard Redner. Note on the consistency of the maximum likelihood estimate for nonidentifiable 548 distributions. *The Annals of Statistics*, 9(1):225–228, 1981. ISSN 00905364. URL <http://www.jstor.org/stable/2240890>.

549

550 [36] Ronald P. Schuyler, Conner Jackson, Josselyn E. Garcia-Perez, Ryan M. Baxter, Sidney Ogolla, Rosemary Rochford, Debashis Ghosh, Pratyaydipta Rudra, and Elena W. Y. Hsieh. Minimizing Batch 551 Effects in Mass Cytometry Data. *Frontiers in Immunology*, 10:2367, October 2019. ISSN 1664-3224.

552 doi: 10.3389/fimmu.2019.02367.

A semi-supervised Bayesian mixture modelling approach for joint batch correction and classification

553 [37] Daniel Stadlbauer, Fatima Amanat, Veronika Chromikova, Kaijun Jiang, Shirin Strohmeier,
554 Guha Asthagiri Arunkumar, Jessica Tan, Disha Bhavsar, Christina Capuano, Ericka Kirkpatrick, Philip
555 Meade, Ruhi Nichalle Brito, Catherine Teo, Meagan McMahon, Viviana Simon, and Florian Kram-
556 mer. SARS-CoV-2 Seroconversion in Humans: A Detailed Protocol for a Serological Assay, Antigen
557 Production, and Test Setup. *Current Protocols in Microbiology*, 57(1):e100, 2020. ISSN 1934-8533.
558 doi: 10.1002/cpmc.100.

559 [38] A. Voller, D. Bidwell, G. Huldt, and E. Engvall. A microplate method of enzyme-linked immunosor-
560 bent assay and its application to malaria. *Bulletin of the World Health Organization*, 51(2):209, 1974.

561 [39] Brian W. Whitcomb, Neil J. Perkins, Paul S. Albert, and Enrique F. Schisterman. Treatment of Batch in
562 the Detection, Calibration, and Quantification of Immunoassays in Large-scale Epidemiologic Studies.
563 *Epidemiology (Cambridge, Mass.)*, 21(Suppl 4):S44–S50, July 2010. ISSN 1044-3983. doi: 10.1097/
564 EDE.0b013e3181dceac2.

A semi-supervised Bayesian mixture modelling approach for joint batch correction and classification: Supplementary material

Stephen Coleman^{1,*}
stephen.coleman@mrc-bsu.cam.ac.uk
Kath Nicholls^{1,2},
kcn25@cam.ac.uk
Xaquin Castro Dopico³
xaquin.castro.dopico@ki.se
Gunilla B. Karlsson Hedestam³
gunilla.karlsson.hedestam@ki.se
Paul D.W. Kirk^{1,2,4,†}
paul.kirk@mrc-bsu.cam.ac.uk
Chris Wallace^{1,2,†}
caw54@cam.ac.uk

¹ MRC Biostatistics Unit

² Cambridge Institute of Therapeutic Immunology & Infectious Disease

⁴ Cancer Research U.K. Cambridge Centre, Ovarian Cancer Programme
University of Cambridge, U.K.

³ Department of Microbiology, Tumor and Cell Biology
Karolinska Institutet, Sweden.

* Corresponding author.

† These authors provided an equal contribution.

Abstract

Description of the model, our choice of priors, and the sampling algorithm. Example of likelihood trace plots for model convergence. Description of how the simulated data is generated for both the main simulation study and the pseudo-ELISA simulation.

1 Model

Our data $X = (X_1, \dots, X_N)$ is generated across B batches where the origin batch of each point is known and represented by the vector $b = [b_1, \dots, b_N]^\top$. We are interested in classifying X into K disjoint classes. We model X using a K component mixture model:

$$p(X|b_n = b, \theta, z) = \sum_{k=1}^K \pi_k f(X_n|\theta_k, z_b). \quad (1)$$

Here $f(\cdot)$ is the density function, $\pi = [\pi_1, \dots, \pi_K]^\top$ are the component or class weights, $\theta = (\theta_1, \dots, \theta_K)$ are the parameters describing the classes and $z = (z_1, \dots, z_B)$ are the parameters associated with the batches. We introduce an allocation variable, $c = [c_1, \dots, c_N]^\top$, to represent the class membership and assume that each class is represented by a single component of the mixture. Conditioning on c , our

model is then

$$p(X_n|b_n = b, c_n = k, \theta, z) = f(X_n|\theta_k, z_b). \quad (2)$$

In our motivating example, c contains some observed values (alternatively, c contains missing values), this enables supervised or semi-supervised methods to infer the missing values. We introduce a binary vector, $\phi = [\phi_1, \dots, \phi_N]^\top$, indicating if the label of the n^{th} individual is observed or not. If we separate our dataset into subsets of labelled and unlabelled data

$$X_l = \{X_n \in X : \phi_n = 1\}, \quad (3)$$

$$X_u = \{X_n \in X : \phi_n = 0\}. \quad (4)$$

and use X_l to train some classifier which predicts the labels of X_u (as we do with the off-the-shelf ML models in our simulation study), our method would be a supervised classifier. However, the Bayesian framework enables us to integrate these steps in a semi-supervised model, using the inferred allocations to include X_u in modelling the class and batch parameters.

1.1 Multivariate Normal

Let f be the density function for the multivariate normal distribution, parametrised by a mean vector μ and a covariance matrix Σ .

We assume

$$\begin{aligned} X_n|c_n, b_n, \dots &\sim \mathcal{N}(\mu_{c_n} + m_{b_n}, \Sigma_{c_n} \oplus S_{b_n}), \\ \implies p(X_n|\cdot) &= [(2\pi)^P |\Sigma_{c_n} \oplus S_{b_n}|]^{-1/2} \\ &\times \exp \left\{ -\frac{1}{2} [X_n - (\mu_{c_n} + m_{b_n})]^T (\Sigma_{c_n} \oplus S_{b_n})^{-1} [X_n - (\mu_{c_n} + m_{b_n})] \right\}. \end{aligned}$$

We also assume that the batch effects have no correlation across dimensions. We restrict the covariance matrix, S_b , to being diagonal and assume independence between the entries of m_b .

Our hierarchical model is

$$\mu_k, \Sigma_k | \xi, \kappa, \nu, \Psi \sim \mathcal{N} \left(\mu_k | \xi, \frac{\Sigma_k}{\kappa} \right) \mathcal{IW}(\Sigma_k | \nu, \Psi), \quad (5)$$

$$m_{b,p} | \lambda, \delta^2 \sim \mathcal{N}(0, \lambda \delta^2), \quad (6)$$

$$(S_b)_{p,p} | \alpha, \beta, S_{loc} \sim \mathcal{IG}(\alpha, \beta, S_{loc}), \quad (7)$$

$$\pi | \gamma \sim Dir(\gamma/K, \dots, \gamma/K), \quad (8)$$

$$c_n | \pi \sim Cat(\pi), \quad (9)$$

$$X_n | c_n = k, b_n = b, \mu_k, \Sigma_k, m_b, S_b \sim \mathcal{N}(\mu_k + m_b, \Sigma_k \oplus S_b). \quad (10)$$

\mathcal{IW} denotes the inverse-Wishart distribution, \mathcal{IG} denotes the inverse-Gamma distribution with a shape α , rate β and location S_{loc} . \mathcal{N} is the Gaussian distribution, Dir is the Dirichlet distribution and Cat is the categorical distribution. As we assume independence of batch effects across dimensions, we model each entry of the b^{th} batch mean vector, $m_{b,p}$, and the b^{th} batch covariance matrix, $(S_b)_{p,p}$, using one dimensional distributions.

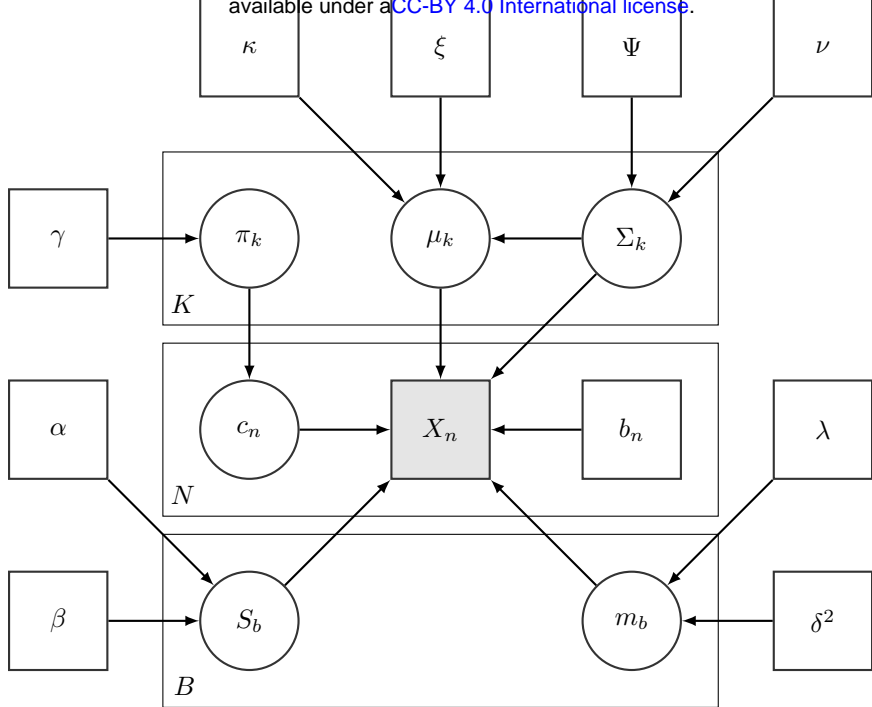


Figure 1: Directed acyclic graph for mixture of multivariate normal distributions with random effects. Squares indicate observed or known quantities. Note that a subset of c is observed in our application.

The total joint probability is

$$\begin{aligned}
p(X, \mu, \Sigma, m, S, \pi, c | b) &= p(\pi | \gamma) p(X, c | \mu_k, \Sigma_k, m_b, S_b, b) \\
&\quad \times \prod_{k=1}^K p(\mu_k | \xi, \Sigma_k, \kappa) p(\Sigma_k | \nu, \Psi) \\
&\quad \times \prod_{b=1}^B \prod_{p=1}^P p(m_{b,p} | \lambda, \delta^2) p((S_b)_{p,p} | \alpha, \beta, S_{loc}) \\
&= f_{Dir}(\gamma) \prod_{n=1}^N \sum_{k=1}^K \pi_k f_{\mathcal{N}}(X_n | \mu_k + m_b, \Sigma_k \oplus S_b) \\
&\quad \times \prod_{k=1}^K f_{\mathcal{N}}(\mu_k | \xi, \Sigma_k, \kappa) f_{\mathcal{IW}}(\Sigma_k | \nu, \Psi) \\
&\quad \times \prod_{b=1}^B \prod_{p=1}^P f_{\mathcal{N}}(m_{b,p} | 0, \lambda \delta^2) f_{\mathcal{IG}}((S_b)_{p,p} | \alpha, \beta, S_{loc}).
\end{aligned}$$

1.2 Multivariate t

If we let f be the density function for the multivariate t (MVT) distribution, parametrised by a mean vector μ , a covariance matrix Σ and degrees of freedom, η , then the model remains as described in section 1.1 and equations 5, except the model likelihood changes and we introduce a prior distribution over η :

$$\eta_k \sim \mathcal{G}(\epsilon, \zeta), \quad (11)$$

$$X_n | c_n = k, b_n = b, \mu_k, \Sigma_k, \eta_k, m_b, S_b \sim t_{\eta_k}(\mu_k + m_b, \Sigma_k \oplus S_b). \quad (12)$$

here \mathcal{G} denotes the Gamma distribution parametrised by a shape and rate.

$$\begin{aligned}
p(X, \mu, \Sigma, \eta, m, S, \pi, c|b) &= p(\pi|\gamma)p(X, c|\mu_k, \Sigma_k, m_b, S_b, b, \eta_k) \\
&\quad \times \prod_{k=1}^K p(\mu_k|\xi, \Sigma_k, \kappa)p(\Sigma_k|\nu, \Psi)p(\eta_k|\epsilon, \zeta) \\
&\quad \times \prod_{b=1}^B \prod_{p=1}^P p(m_{b,p}|\lambda\delta^2)p((S_b)_{p,p}|\alpha, \beta, S_{loc}) \\
&= f_{Dir}(\gamma) \prod_{n=1}^N \sum_{k=1}^K \pi_k f_t(X_n|\mu_k + m_b, \Sigma_k \oplus S_b, \eta_k) \\
&\quad \times \prod_{k=1}^K f_{\mathcal{N}}(\mu_k|\xi, \Sigma_k, \kappa) f_{\mathcal{IW}}(\Sigma_k|\nu, \Psi) f_{\mathcal{G}}(\eta_k|\epsilon, \zeta) \\
&\quad \times \prod_{b=1}^B \prod_{p=1}^P f_{\mathcal{N}}(m_{b,p}|0, \delta^2) f_{\mathcal{IG}}((S_b)_{p,p}|\alpha, \beta, S_{loc}).
\end{aligned}$$

1.3 Parameter interpretation

Note that the ‘‘batch’’ parameters should not be inferred as direct estimates of the effect the batches have on the true measures. As we are essentially performing a classification on the inferred batch-free dataset,

$$(Y_{n,p}|c_n = k, b_n = b, \dots) = \frac{X_{n,p} - m_{b,p} - \mu_{k,p}}{(S_b)_{p,p}} + \mu_{k,p}, \quad (13)$$

$$p(Y_n|\mu, \Sigma, \pi_k) = \sum_{k=1}^K \pi_k p(Y_n|\mu_k, \Sigma_k), \quad (14)$$

and the likelihood parameters of $\mu_k + m_b$ and $\Sigma_k \oplus S_b$ are not constrained in the likelihood, we recommend that users focus on the relative change in the measurements for batches, the inferred dataset and the inferred classification rather than the direct meaning of individual parameters.

2 Empirical Bayes

We use the suggestions of Fraley and Raftery (2007) for our choices of prior hyperparameters on the class parameters.

$$\xi = \frac{1}{N} \sum_{n=1}^N X_n, \quad (15)$$

$$\kappa = 0.01, \quad (16)$$

$$\nu = P + 2. \quad (17)$$

The choice of ξ is self-explanatory. κ can be viewed as the number of observations contributing to the prior. Fraley and Raftery (2007) choose a value based on experiments to acquire a BIC curve that is a smooth extension of the counterpart without a prior. The marginal prior distribution of μ_k is a Student’s t distribution centred at ξ with $\nu - P + 1$ degrees of freedom. ν is the smallest integer value for the degrees of freedom that gives a finite variance.

We set Ψ as a diagonal matrix. Let

$$\Sigma_0 = \frac{1}{N-1} \sum_{n=1}^N (X_n - \xi)(X_n - \xi)^T, \quad (18)$$

$$\bar{\sigma}_0^2 = \frac{1}{P} \sum_{p=1}^P (\Sigma_0)_{p,p}, \quad (19)$$

then

$$\Psi_{p,p} = \frac{\bar{\sigma}_0^2}{K^{2/P}}. \quad (20)$$

The logic is that the mixture components are expected, *a priori*, to each fill a common fraction of the total volume of space the data occupies.

For the concentration on the class weights, we use a flat prior with $\gamma = 1$. In our motivating example of ELISA data, we cannot use more information (such as the ratio of class members in the known data), as the negative controls are historical samples the number of which is chosen before the experiment and is not related to the expected seroprevalence in the dataset.

For the degrees of freedom for the MVT, η_k , we use an uninformative prior that offers a range of plausible values, $\epsilon = 2.0$, $\zeta = 0.1$ (Juárez and Steel, 2010).

3 Sampling algorithm

We use a *Metropolis-within-Gibbs* algorithm to sample our parameters. All parameters where the form of their posterior distribution is known are sampled via Gibbs sampling (Geman and Geman, 1984), the remaining parameters are sampled in a Metropolis-Hastings step (Metropolis et al., 1953; Hastings, 1970).

Algorithm 1: *sampler*($X, I, c_0, fixed, b, K$)

Input:

Data X ,

The number of iterations, I ,

Initial classification, c_0 ,

Fixed labels, $fixed$,

Batch membership, b ,

The number of classes to model, K ,

The prior distributions for each parameter,

The likelihood function, $p(X|\cdot)$,

The proposal distributions for each class and batch parameter, $q(\theta)$.

Output: A Markov chain of accepted values for each of the sampled parameters.

begin

```

/* initialise parameters by drawing from the prior */  

sampleFromPriors();  

for i = 1 to I do
    /* Update the class weights in a Gibbs step */  

    π ← updateWeights(c, γ);  

    /* Update the class and batch parameters in a Metropolis-Hastings step */  

    for k = 1 to K do
        Σik ← metropolisHastings(Σi-1k, νΣ, qΣ(·));  

        μik ← metropolisHastings(μi-1k, σ2μ I, qμ(·));  

        for b = 1 to B do
            for p = 1 to P do
                (Sib)p,p ← metropolisHastings((Si-1b)p,p, βS, qS(·));  

                mib ← metropolisHastings(mi-1b, σ2m I, qm(·));  

            /* Update the class allocations */  

            c ← updateAllocations(X, b, π, fixed);  

            /* Update the batch corrected data based on the current parameters. */  

            Y ← batchCorrected(X, c, b, μ, m, S);

```

3.1 Proposal distributions

For our batch and class parameters, we choose proposal densities that have an expectation of the current value and have the correct support. The class and batch means have a support (∞, ∞) ; this allows use

Algorithm 2: *sampleFromPriors()*

Output: Initial values for class and batch parameters.

begin

```

for  $k = 1$  to  $K$  do
   $\Sigma_k \sim \mathcal{IW}(\nu, \Psi);$ 
   $\mu_k \sim \mathcal{N}(\xi, \Sigma_k/\kappa);$ 
for  $b = 1$  to  $B$  do
  for  $p = 1$  to  $P$  do
     $(S_b)_{p,p} \sim \mathcal{IG}(\alpha, \beta, S_{loc});$ 
     $m_{b,p} \sim \mathcal{N}(0, \delta^2);$ 

```

Algorithm 3: *updateAllocation($X, b, \pi, fixed$)*

Input:

X , the observed data,
 b , the batch variable,
 π , the class weights,
 $fixed$, the binary vector indicating if the label is known.

Output: c , a new allocation vector.

begin

```

for  $n = 1$  to  $N$  do
  /* If the item's class is unknown, update. */
  if  $fixed_n == 0$  then
     $ll \leftarrow logLikelihood(X_n, b_n);$ 
     $ll \leftarrow ll + \log \pi;$ 
    /* Handle overflow and normalise.
     $ll \leftarrow \exp(ll - \max(ll));$ 
     $ll \leftarrow ll / \sum(ll);$ 
    /* update class.
     $u \sim \mathcal{U}(0, 1);$ 
     $c_n \leftarrow \sum(u > cumsum(ll));$ 

```

Algorithm 4: *updateWeights(c, γ)*

Input:

c , the current allocation,
 γ , the prior concentration vector for the class weights.

Output: π , a new class weight vector.

begin

```

for  $k = 1$  to  $K$  do
   $members_k \leftarrow which(c == k);$ 
   $N_k \leftarrow count(members_k);$ 
  /* the concentration for  $\pi_k$  is the sum of the count of class members and
  the prior concentration. */
   $\gamma \leftarrow \gamma_k + N_k;$ 
   $\pi_k \sim \mathcal{G}(\gamma, 1.0);$ 
  /* convert the weights from a Gamma random variable to a Dirichlet (or, if
   $K = 2$ , a Beta) random variable. */
   $\pi \leftarrow \pi / sum(\pi);$ 

```

Algorithm 5: $batchCorrected(X, c, b, \mu, m, S)$

Input:

X , the observed dataset,
 c , the allocation vector,
 b , the batch label vector,
 μ , the class means,
 m , the batch effect on the class means,
 S , the batch effect on the class standard deviations.

Output: Y , the batch-corrected dataset.

begin

```

/* Iterative over points performing batch correction. */
for n = 1 to N do
    /* Extract the current point's class and batch. */
    k ← cn;
    b ← bn;
    /* Remove the inferred batch effect. */
    for n = 1 to N do
        Yn,p ← (Xn,p − μk,p − mb,p)/(Sb)p,p + μk,p;

```

Algorithm 6: $metropolisHastings(\theta, \sigma_{win}^2, q(\cdot))$

Input:

Current parameter value θ ,
Proposal window, σ_{win}^2 ,
The proposal distribution, $q(\theta, \sigma_{win}^2)$,
The prior distribution for θ , $p(\theta)$,
The likelihood of θ , $p(X|\theta)$.

Output: A value θ^* .

begin

```

/* sample a proposal for θ
θ' ~ q(θ, σwin2);
/* calculate the acceptance probability (note that if q(·) is a symmetric
distribution it cancels out)
α ← min (1,  $\frac{p(X|\theta')p(\theta')q(\theta|\theta')}{p(X|\theta)p(\theta)q(\theta'|\theta)}$ );
u ~ Unif(0, 1);
if u < α then
    θ* ← θ';
else
    θ* ← θ;

```

of a Gaussian proposal distribution with a mean of the current value.

$$m_b^* \sim \mathcal{N}(m_b, \sigma_m^2 \mathbf{I}), \quad (21)$$

$$\mu_k^* \sim \mathcal{N}(\mu_k, \sigma_\mu^2 \mathbf{I}). \quad (22)$$

This density is symmetric and the relationship between the acceptance rate and the choice of the proposal window (σ_m^2 and σ_μ^2) is relatively intuitive, the acceptance rate will decrease as the window increases.

The batch standard deviations have a support of (S_{loc}, ∞) . To ensure that proposed values remain in this range we use a Gamma proposal distribution with a shape of the current value divided by the rate, the rate set to some constant and a location of S_{loc} .

$$(S_b^*)_{p,p} \sim \mathcal{G}((S_b)_{p,p}/\beta_S, \beta_S, S_{loc}). \quad (23)$$

This proposal has an expected value of $(S_b)_{p,p}$. However, it is asymmetric and the acceptance rate increases as β_S increases. We propose all P members of S_b in each sampling step.

The class covariance matrices are the most difficult to sample. There are P^2 values to propose and must be positive semi-definite. We use a Wishart proposal to satisfy this

$$\Sigma_k^* \sim \mathcal{W}(\nu_\Sigma, \Sigma_k). \quad (24)$$

All of the proposal windows, $(\sigma_\mu^2, \sigma_m^2, \beta_S, \nu_\Sigma)$, are tuned aiming to achieve acceptance rates in the range $[0.1, 0.5]$ (Roberts and Rosenthal, 2001); if this is not possible we prioritise keeping acceptance rates above 0.1. This can involve multiple tuning runs of the sampler on each dataset.

4 Simulation study

We use a simulation study to test the model behaviour in examples where the generating model and the true labelling are known. We aim to explore

- the batch effects inferred by the model when none are present.
- the sampled distributions of the degree of freedom parameters in the mixture of multivariate t distributions.
- how the model behaves when there is some sort of inequality in the batches, e.g.,
 - different batch sizes,
 - different class representation in each batch, and
 - large difference in the magnitude of batch effects.
- how the model handles misspecification.

4.1 Design

Our study uses six different scenarios to test and benchmark behaviour. We use a *Base case* as the default scenario that each other scenario is a variation of. For example, the *No batch effects* scenario is the Base case with the batch means set to 0 and the batch standard deviations set to 1.0. We define each scenario by a set of parameters

- N : the number of rows in the dataset,
- P : the number of features in the dataset,
- K : the number of classes in the dataset,
- B : the number of batches in the dataset,
- $\Delta\mu_{k,p}$: the cluster means before the batch effects,
- $\sigma_{k,p}$: the cluster standard deviations before batch effects,
- π_k : the expected class representations,
- m_b : the batch effect on the means,
- S_b : the batch effect on the standard deviations,
- w_b : the expected proportion of the dataset in each batch.

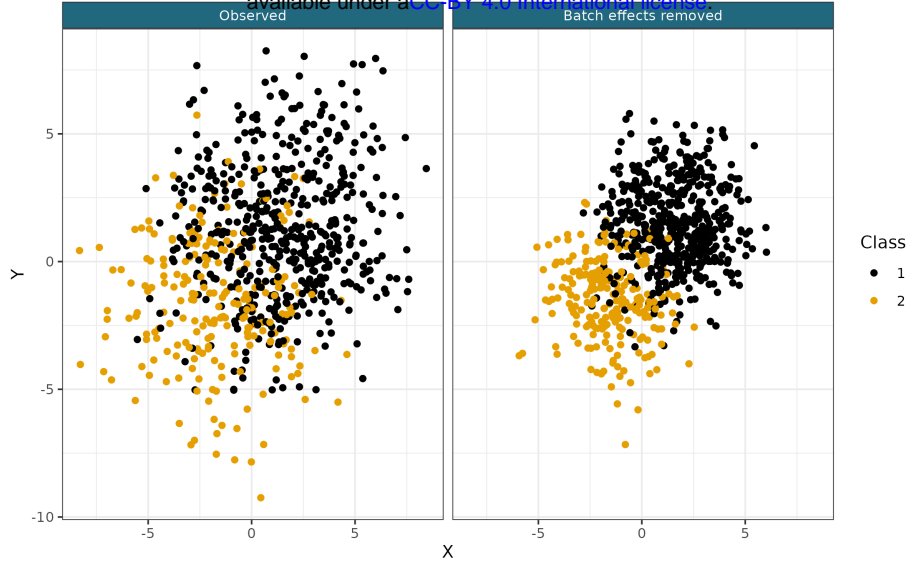


Figure 2: Example of a generated dataset from the Base case scenario.

We use the distance between cluster means in a single dimension, as this is the quantity of interest rather than specific values of μ_k .

To generate the datasets, we first sample batch and class labels based on w_b and π_k respectively. The measurements for each point are then generated from a Gaussian distribution defined by these labels (except in the *multivariate t generated* scenario where the generating distribution is the eponymous distribution). We use a diagonal covariance matrix for simplicity. Each column generated randomly permutes the parameters associated with each class and batch; this means that the different columns can contain different information.

$$b_n \sim \text{Cat}(w), \quad (25)$$

$$c_n \sim \text{Cat}(\pi), \quad (26)$$

$$Y_n \sim \mathcal{N}(\mu_{c_n}, \Sigma_{c_n}), \quad (27)$$

$$X_n \sim \mathcal{N}(Y_n + m_{b_n}, S_{b_n}). \quad (28)$$

4.1.1 Base case

The parameters defining each simulation in the scenario are

$$\begin{aligned} N &= 750, \\ P &= 2, \\ K &= 2, \\ B &= 5, \\ \Delta\mu_{k,p} &= 3, \\ \sigma_{k,p} &= 1.6, \\ \pi^T &= (0.70, 0.30), \\ m_b &= (-1)^b 0.75, \\ S_b &\in \{1.3, 1.7\}, \\ w_b &= \frac{1}{5}. \end{aligned}$$

All the scenarios used these same parameters unless explicitly stated otherwise.

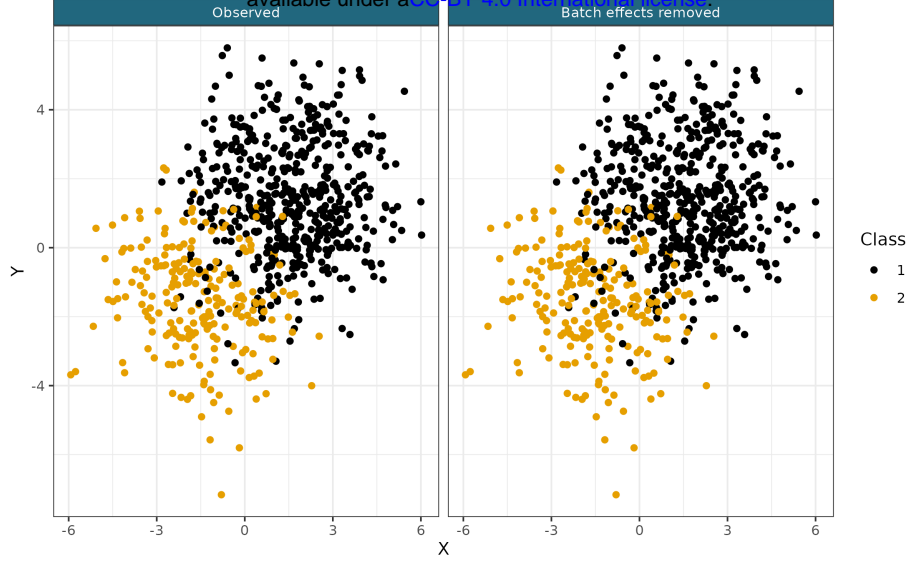


Figure 3: Example of a generated dataset from the No batch effects scenario. Note that the dataset is identical before and after batch-correction.

4.1.2 No batch effects

This scenario is aimed at measuring the bias of the inferred batch effects. We remove the batch effects from the generating model by using values

$$m_b = 0.0,$$

$$S_b = 1.0.$$

Note the inferred values of S are restricted to the open interval $(1, \infty)$ in our sampler. Because of this we hope that the sampled batch scaling effect has a similar distribution across all batches rather than sampling a distribution centred on 1.0.

4.1.3 Varying batch size

This scenario investigates the behaviour of the model when the batch sizes are very different.

$$w^T = \left(\frac{1}{2}, \frac{1}{4}, \frac{1}{8}, \frac{1}{16}, \frac{1}{16} \right). \quad (29)$$

4.1.4 Varying batch effects

This scenario tests how successfully the model infers to differing batch effects in each batch, different magnitudes of batch effects (with some in the tails of the prior distribution) and the direction of the batch mean shift.

$$m_{b,p} \in [-1.5, -0.5, 0.0, 0.5, 1.5], \quad (30)$$

$$(S_b)p, p \in [1.0, 1.25, 1.50, 1.75, 2.25]. \quad (31)$$

4.1.5 Varying class representation across batches

In this scenario we investigate how the model responds to different expected representation of classes in each batch. This scenario might apply if the batches are collected across time and the proportion of each class in the population is expected to fluctuate. In this case the expected class proportions vary across batches are therefore a $K \times B$ matrix,

$$\pi = \begin{pmatrix} 0.75 & 0.60 & 0.50 & 0.30 & 0.15 \\ 0.25 & 0.40 & 0.50 & 0.70 & 0.85 \end{pmatrix}. \quad (32)$$

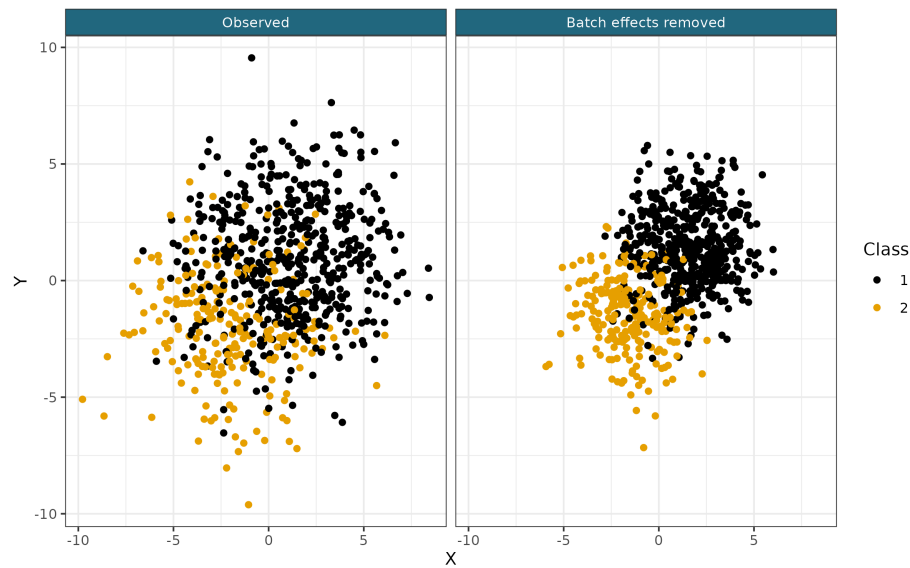


Figure 4: Example of a generated dataset from the Varying batch size scenario.

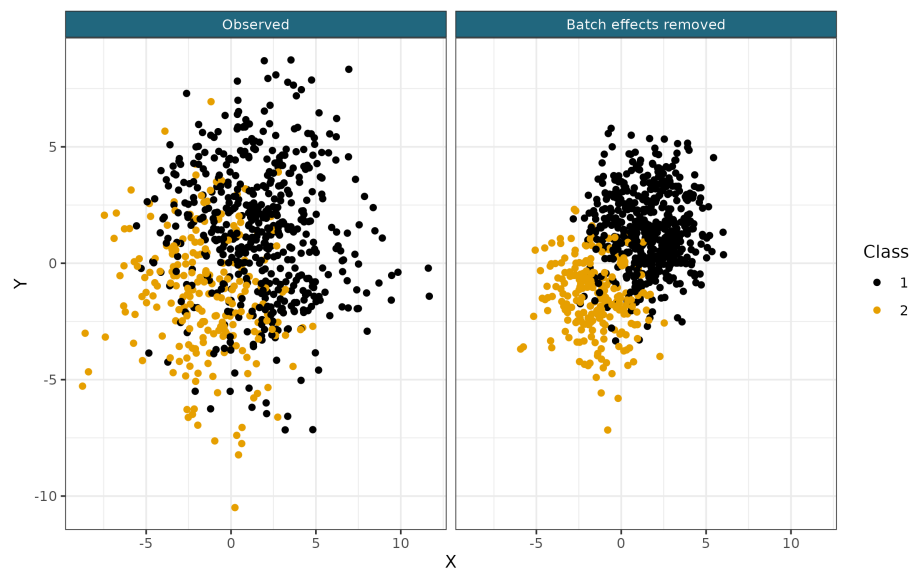


Figure 5: Example of a generated dataset from the Varying batch effects scenario.

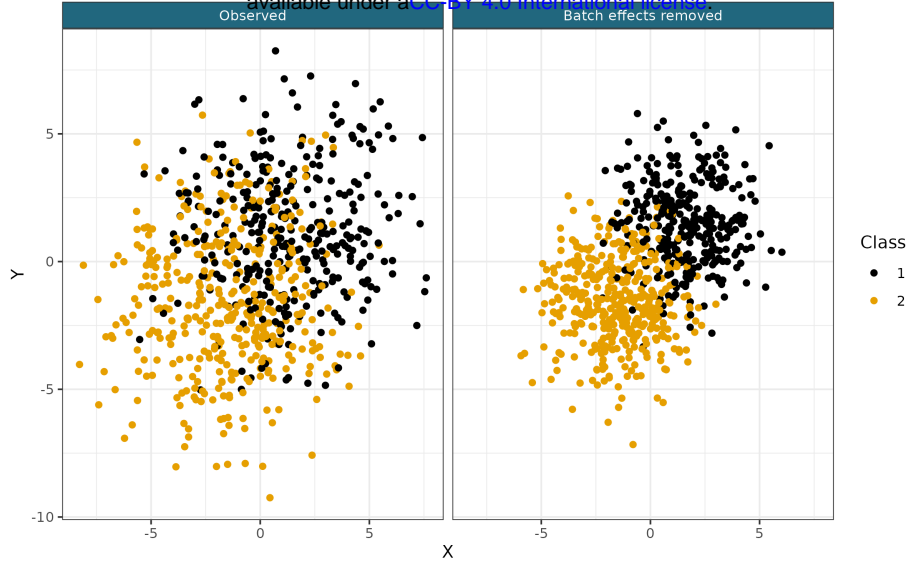


Figure 6: Example of a generated dataset from the Varying class representation across batches scenario.

In each batch one column of this matrix is used to sample the class membership. This introduces a dependency for c_n on b_n , i.e.,

$$(c_n|b_n = b, \pi) \sim \text{Cat}(\pi_b). \quad (33)$$

4.1.6 Multivariate t generated

This scenario generates the data for each class from a multivariate t (**MVT**) distribution. This type of data is believed to be common in biology and we wish to investigate how well the model learns the degrees of freedom parameter and to compare the performance of the mixture of Gaussians model to the mixture of MVTs model.

$$Y_n|c_n = k \sim t_{\eta_k}(\mu_k, \Sigma_k), \quad (34)$$

$$\nu = (4, 7). \quad (35)$$

4.1.7 Log-poisson generated

This scenario generates the data for each class from a Poisson distribution distribution, which is then log-transformed and has some Gaussian noise added. This type of data is believed to be common in biology where count data is so prolific and we wish to investigate how well the model behaves when it is strongly misspecified.

$$(Y_{n,p}|c_n = k, \dots) \sim \text{Pois}(\lambda_{k,p}), \quad (36)$$

$$(\varepsilon_{n,p}|b_n = b, \dots) \sim \text{Pois}(\lambda_{b,p}), \quad (37)$$

$$X_{n,p}^* = Y_{n,p} + \varepsilon_{n,p}, \quad (38)$$

$$\epsilon_{n,p} \sim \mathcal{N}(0, 1), \quad (39)$$

$$X_{n,p} = \log(X_{n,p}^*) + \epsilon_{n,p}, \quad (40)$$

for all $n = 1, \dots, N, p = 1, \dots, P$, with X being the modelled data.

4.1.8 High-dimensional

The data are generated from a mixture of MVN distributions as in the Base case, but more features ($P = 15$) are generated. To compensate for the additional information these contain, the distance between the class means in each feature is reduced.

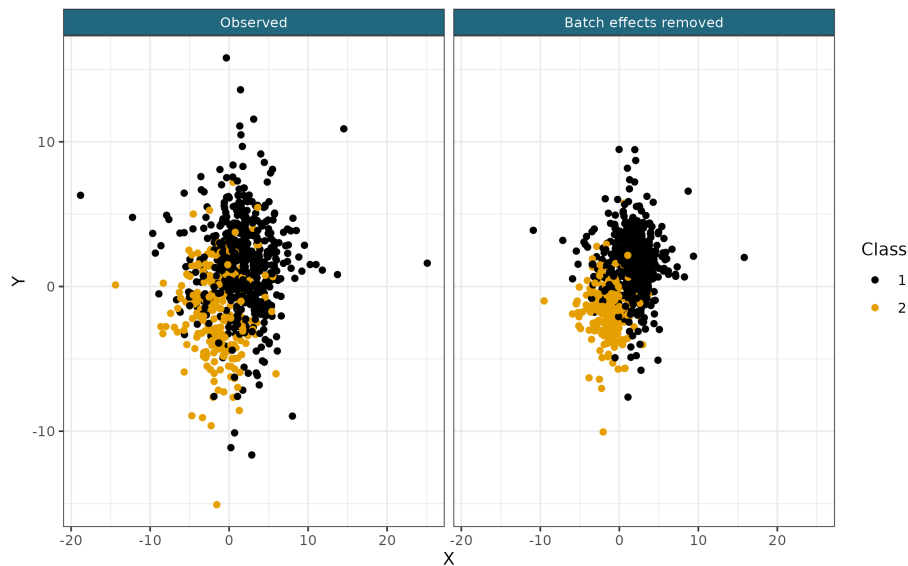


Figure 7: Example of a generated dataset from the MVT scenario.

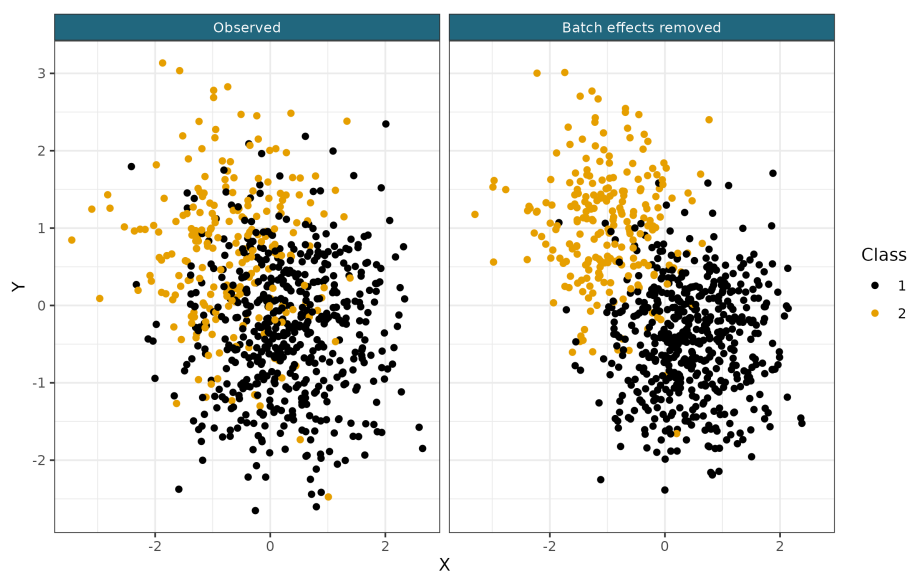


Figure 8: Example of a generated dataset from the Log-Poisson scenario.



Figure 9: Example of a generated dataset from the High-dimensional scenario. Samples being clustered in rows, measurements in columns.

4.1.9 Hardest

This scenario uses the class / batch dependency of Varying class representation across batches scenario, the data generating mechanism of the Log-poisson generated scenario and the dimensionality of the High-dimensional scenario.

4.2 Additional results

5 Gene expression data

The batch labels, $b = [b_1, \dots, b_N]^\top$, $N = 242$, are generated according to one of two scenarios described below, and then used to add batch-effects to the gene expression data.

5.1 Scenario a) No dependency between class and batch

$$B = 4, \quad (41)$$

$$w \sim \text{Dirichlet}(10), \quad (42)$$

$$b_n \sim \text{Categorical}(w). \quad (43)$$

5.2 Scenario b) Class and batch are dependent

$$B = 4, \quad (44)$$

$$w = \begin{pmatrix} 0.6 & 0.2 & 0.15 & 0.05 \\ 0.2 & 0.7 & 0.1 & 0.0 \\ 0.0 & 0.2 & 0.6 & 0.2 \\ 0.1 & 0.2 & 0.7 & 0.0 \\ 0.2 & 0.2 & 0.2 & 0.4 \\ 0.2 & 0.1 & 0.1 & 0.6 \end{pmatrix}, \quad (45)$$

$$(b_n | c_n = k) \sim \text{Categorical}(w_k^\top). \quad (46)$$

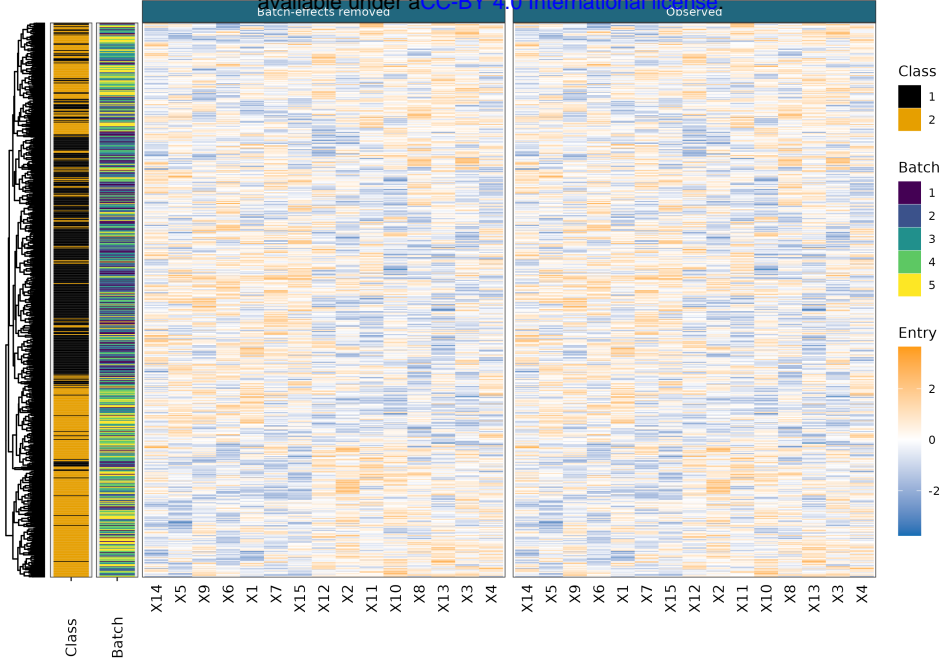


Figure 10: Example of a generated dataset from the Hardest scenario. Samples being clustered in rows, measurements in columns.

5.3 Batch-effects

Given the batch of origin, we then simulate batch parameters

$$m_{b,p} \sim \mathcal{N}(0, 0.1^2), \quad (47)$$

$$\log(S_{b,p}) \sim \mathcal{N}(-0.5, 0.3^2), \quad (48)$$

$$(\epsilon_{n,p} | b_n = b) \sim \mathcal{N}(m_{b,p}, S_{b,p}), \quad (49)$$

$$X_{n,p} = Y_{n,p} + \epsilon_{n,p}, \quad (50)$$

where $X = (X_1, \dots, X_N)$ is the modelled data, $Y = (Y_1, \dots, Y_N)$ is the gene expression data as represented in its first four principal components and $n = 1, \dots, 242$ and $p = 1, \dots, 4$.

6 Model convergence

For the simulated data we use the Geweke diagnostic for the complete log-likelihood after burn-in to assess within-chain convergence. We obtain a p -value by transforming the absolute value of the Z -scores with the Gaussian cumulative distribution function. We then discard all chains which have p -values below a threshold of 0.05. From the remaining chains we use that which has the highest median complete log-likelihood.

For the real data we visually inspect the complete log-likelihood trace plots and manually select which chains have converged to the same mode in the posterior distribution (possibly the global mode). Performing the entire process manually is feasible for the real datasets as there are less chains. An example of this process is shown in figure 12.

7 Dopico *et al.*

Table 1 shows the seroprevalence estimate for the different methods in the data from Castro Dopico *et al.* (2021).

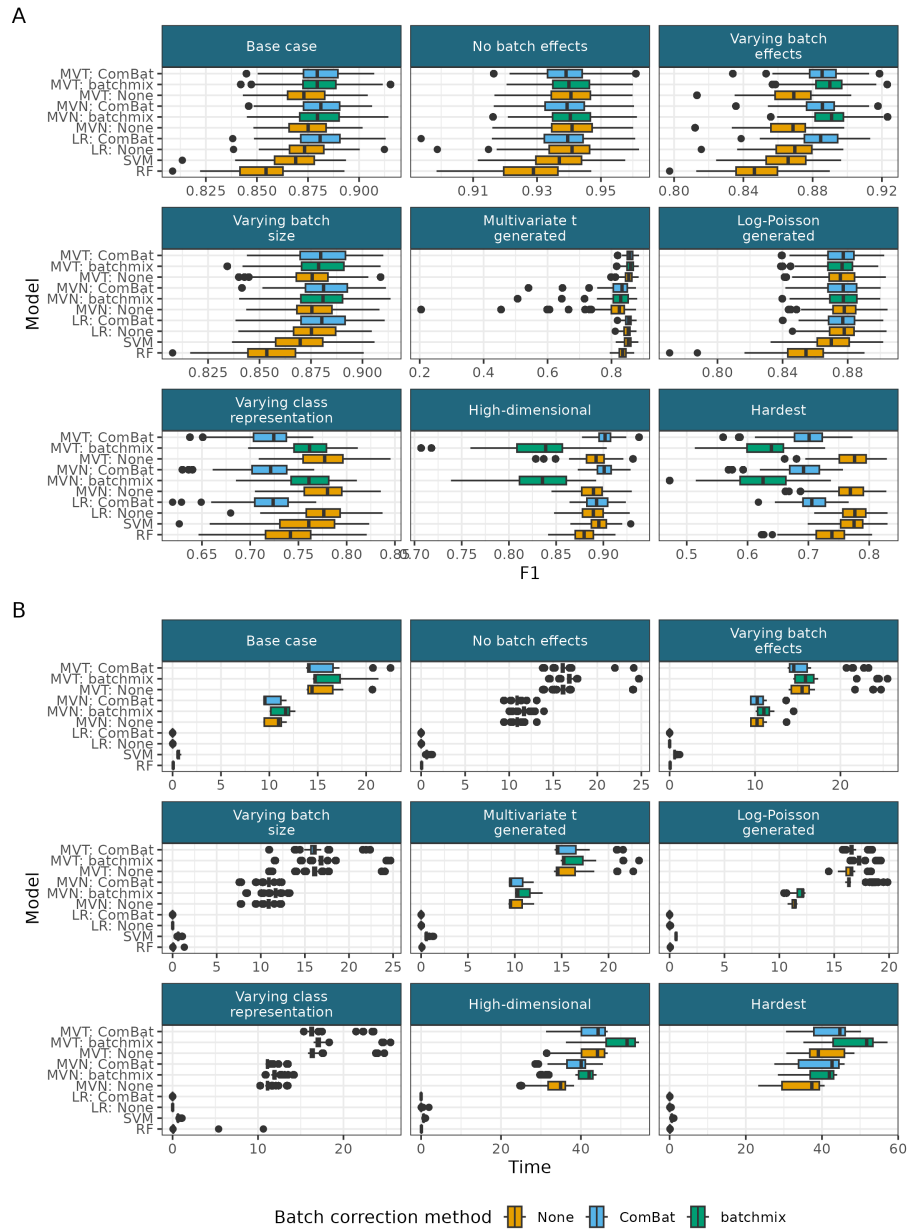


Figure 11: Additional results for the simulation study. A) F1 score for the unlabelled data. B) Time taken for each method.

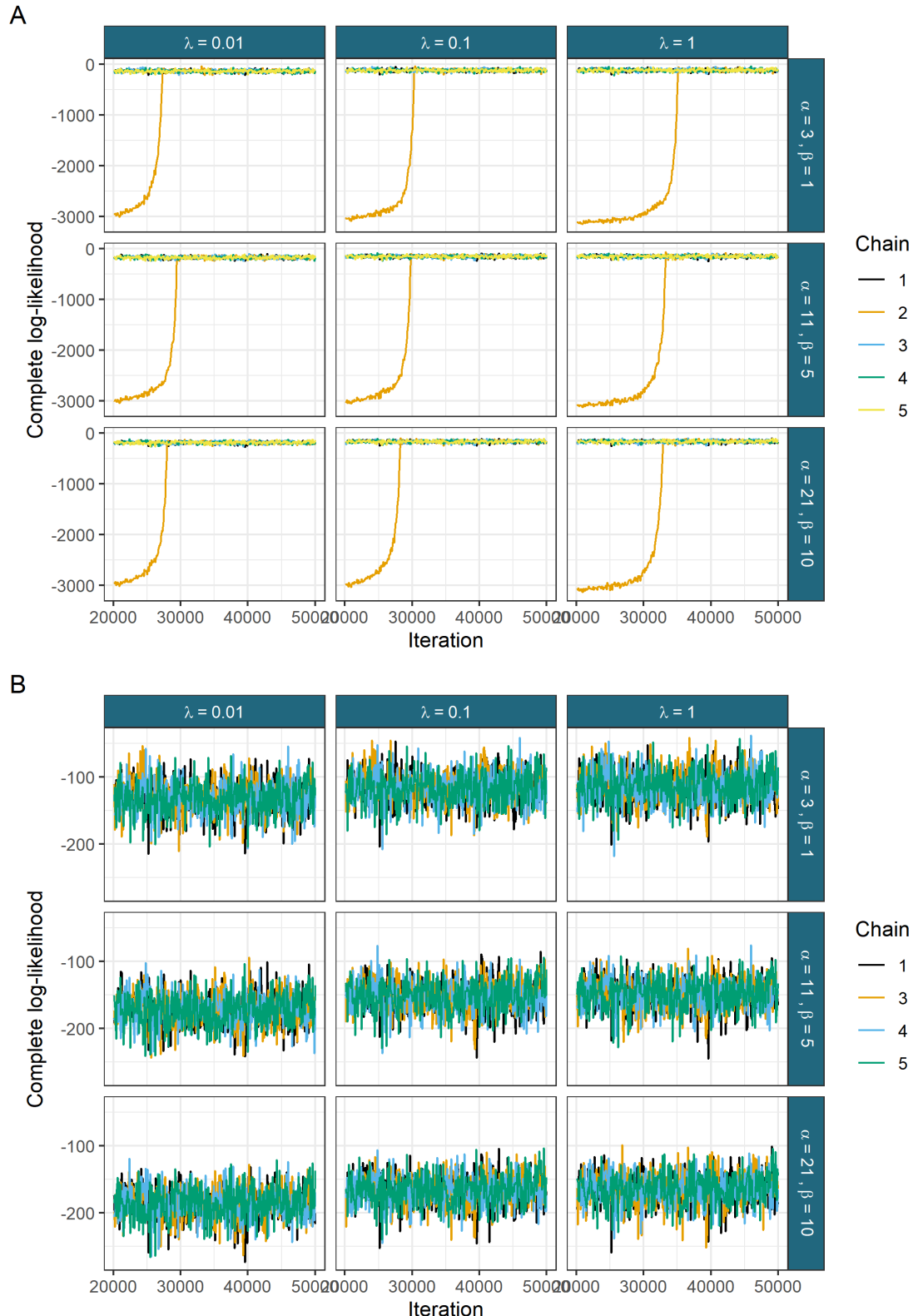


Figure 12: The complete log-likelihood for the MVT model in Stockholm ELISA data for A) all chains and B) the converged chains.

Date	SVM-LDA*	Bayesian learner	MVT	RF	SVM	LR	LR - BC
2020/04/05	NA	2.35	1.60	1.00	1.00	1.00	2.00
2020/04/26	4.26	4.73	4.92	4.50	5.00	5.00	5.00
2020/05/03	4.33	5.34	5.74	4.50	4.50	5.00	5.50
2020/05/10	7.87	5.86	8.87	8.50	8.50	8.50	10.50
2020/05/17	7.36	6.28	8.05	7.50	4.50	8.00	8.50
2020/05/24	7.49	6.64	8.34	8.00	6.50	7.50	9.50
2020/05/31	3.54	6.97	4.15	4.00	3.50	4.00	5.00
2020/06/07	8.41	7.31	9.83	9.50	8.00	10.00	10.50
2020/06/14	6.90	7.75	7.55	7.00	7.00	7.00	8.50
2020/06/21	6.44	8.30	7.80	7.00	6.50	7.50	8.00
2020/07/26	13.20	11.34	16.72	15.00	11.50	16.50	16.00
2020/08/02	9.16	11.79	10.48	9.00	8.50	10.00	10.00
2020/08/09	11.30	12.15	13.43	12.00	8.00	13.00	13.50
2020/08/16	10.84	12.43	12.15	12.00	10.50	11.50	11.00
2020/08/23	12.97	12.65	15.55	15.50	11.00	15.00	15.00
2020/11/08	11.79	14.28	13.72	12.00	11.50	12.50	14.00
2020/11/15	14.20	14.47	18.85	15.50	14.50	17.00	18.50
2020/11/22	13.37	14.72	16.44	15.50	15.50	15.50	16.00
2020/11/29	13.20	14.98	17.36	15.00	15.00	16.00	16.50
2020/12/06	11.52	15.29	14.47	12.50	11.00	13.00	13.50
2020/12/13	15.73	15.64	19.65	18.00	16.00	18.00	19.00

Table 1: Seroprevalence estimates across time for each method in the data from Castro Dopico et al. (2021). The highest estimates at each data are coloured orange, the lowest are coloured blue. * from Castro Dopico et al. (2021).

8 Pseudo-ELISA data

We use the mean posterior values from a converged chain from the MVT mixture model as the parameters to generate the ELISA-like data. For the class parameters, these are:

$$\Sigma_1 = \begin{pmatrix} 0.042 & 0.035 \\ 0.035 & 0.038 \end{pmatrix}, \quad \Sigma_2 = \begin{pmatrix} 0.086 & 0.123 \\ 0.123 & 0.195 \end{pmatrix} \quad (51)$$

$$\mu_2 = \begin{pmatrix} -2.43 \\ -2.43 \end{pmatrix}, \quad \mu_1 = \begin{pmatrix} -0.63 \\ -0.75 \end{pmatrix}, \quad (52)$$

$$\eta_1 = 7.02, \quad \eta_2 = 13.35. \quad (53)$$

and for the batch parameters,

$$S_1 = \begin{pmatrix} 1.28 & 0.0 \\ 0.0 & 1.21 \end{pmatrix}, \quad m_1 = \begin{pmatrix} 0.03 \\ -0.09 \end{pmatrix}, \quad (54)$$

$$S_2 = \begin{pmatrix} 1.86 & 0.0 \\ 0.0 & 1.70 \end{pmatrix}, \quad m_2 = \begin{pmatrix} 0.09 \\ -0.02 \end{pmatrix}, \quad (55)$$

$$S_3 = \begin{pmatrix} 1.36 & 0.0 \\ 0.0 & 1.28 \end{pmatrix}, \quad m_3 = \begin{pmatrix} 0.01 \\ -0.13 \end{pmatrix}, \quad (56)$$

$$S_4 = \begin{pmatrix} 1.21 & 0.0 \\ 0.0 & 1.32 \end{pmatrix}, \quad m_4 = \begin{pmatrix} 0.05 \\ -0.15 \end{pmatrix}, \quad (57)$$

$$S_5 = \begin{pmatrix} 1.58 & 0.0 \\ 0.0 & 1.40 \end{pmatrix}, \quad m_5 = \begin{pmatrix} 0.11 \\ -0.09 \end{pmatrix}, \quad (58)$$

$$S_6 = \begin{pmatrix} 1.20 & 0.0 \\ 0.0 & 1.23 \end{pmatrix}, \quad m_6 = \begin{pmatrix} 0.55 \\ 0.36 \end{pmatrix}, \quad (59)$$

$$S_7 = \begin{pmatrix} 1.25 & 0.0 \\ 0.0 & 1.26 \end{pmatrix}, \quad m_7 = \begin{pmatrix} 0.10 \\ -0.10 \end{pmatrix}. \quad (60)$$

We use the predicted proportion of each batch as our batch-specific class weights,

$$\pi = \begin{pmatrix} 0.95 & 0.87 & 0.91 & 0.88 & 0.96 & 0.10 & 0.95 \\ 0.05 & 0.13 & 0.90 & 0.12 & 0.04 & 0.90 & 0.05 \end{pmatrix}. \quad (61)$$

Each column corresponds to a batch and each row is the class weight. We denote the class weights within a batch (i.e., one of these columns) by π_b . The probability of being drawn from a given batch is simply the observed proportion of items in each batch.

$$w = (0.18 \ 0.18 \ 0.06 \ 0.28 \ 0.15 \ 0.02 \ 0.13). \quad (62)$$

We then generate a batch and class label for each item and then observed measurements conditioning on these labels, specifically for a given item index n :

$$b_n \sim \text{Cat}(w), \quad (63)$$

$$c_n | b_n = b \sim \text{Cat}(\pi_b), \quad (64)$$

$$X_n | c_n = k, b_n = b \sim t_{\eta_k}(\mu_k + m_b, \Sigma_k \oplus S_b). \quad (65)$$

For the seronegative class (we use the label of $c_n = 1$ for this class), the ϕ_n parameter indicating if the n^{th} item has an observed label is a Bernoulli random variable. For the seropositive class we introduce a bias to match the reality that it is more extreme observations that tend to have an observed label. To do this we find the most extreme value in each measurement, denoted X_{max} , (note that X_{max} is unlikely to be an observed value) and calculate the Euclidean distance between this and our observed values. We then sample ϕ according to:

$$p(\phi_n = 1 | c_n = 1) = p(1 - p), \quad (66)$$

$$p(\phi_n = 1 | c_n = 2) = p(1 - p) \exp\{-d(X_n, X_{max})\}, \quad (67)$$

where $p = \frac{1}{3}$. This values is chosen as the proportion of observed labels to the predicted labels is 0.332 for the seronegative class and 0.241 for the seropositive class. Our sampling process finds provides less observed seropositive labels than we have in the real data (the ratio of observed labels to true labels for the seropositive class had a mean of 0.16 across 500 simulated datasets), but we think representing the bias in the positive controls is more important than acquiring the exact proportion of training data.

References

X. Castro Dopico, S. Muschiol, M. Christian, L. Hanke, D. J. Sheward, N. F. Grinberg, J. Rorbach, G. Bogdanovic, G. M. Mcinerney, T. Allander, C. Wallace, B. Murrell, J. Albert, and G. B. Karlsson Hedestam. Seropositivity in blood donors and pregnant women during the first year of SARS-CoV-2 transmission in Stockholm, Sweden. *Journal of Internal Medicine*, May 2021. ISSN 1365-2796. doi: 10.1111/joim.13304.

Chris Fraley and Adrian E Raftery. Bayesian Regularization for Normal Mixture Estimation and Model-Based Clustering. *Journal of Classification*, 24(2):27, September 2007.

Stuart Geman and Donald Geman. Stochastic Relaxation, Gibbs Distributions, and the Bayesian Restoration of Images. *IEEE Transactions on Pattern Analysis and Machine Intelligence*, PAMI-6 (6):721–741, November 1984. ISSN 1939-3539. doi: 10.1109/TPAMI.1984.4767596. Conference Name: IEEE Transactions on Pattern Analysis and Machine Intelligence.

W. K. Hastings. Monte Carlo sampling methods using Markov chains and their applications. *Biometrika*, 57(1):97–109, April 1970. ISSN 0006-3444. doi: 10.1093/biomet/57.1.97. URL <https://doi.org/10.1093/biomet/57.1.97>.

Miguel A. Juárez and Mark F. J. Steel. Model-Based Clustering of Non-Gaussian Panel Data Based on Skew- t Distributions. *Journal of Business & Economic Statistics*, 28(1): 52–66, January 2010. ISSN 0735-0015, 1537-2707. doi: 10.1198/jbes.2009.07145. URL <http://www.tandfonline.com/doi/abs/10.1198/jbes.2009.07145>.

Nicholas Metropolis, Arianna W. Rosenbluth, Marshall N. Rosenbluth, Augusta H. Teller, and Edward Teller. Equation of State Calculations by Fast Computing Machines. *The Journal of Chemical Physics*, 21(6):1087–1092, June 1953. ISSN 0021-9606. doi: 10.1063/1.1699114. URL <https://aip.scitation.org/doi/abs/10.1063/1.1699114>. Publisher: American Institute of Physics.

Gareth O. Roberts and Jeffrey S. Rosenthal. Optimal scaling for various Metropolis-Hastings algorithms. *Statistical Science*, 16(4):351–367, November 2001. ISSN 0883-4237, 2168-8745. doi: 10.1214/ss/1015346320. URL <https://projecteuclid.org/journals/statistical-science/volume-16/issue-4/Optimal-scaling-for-various-Metropolis-Hastings-algorithms>. Publisher: Institute of Mathematical Statistics.